

# **SCDAP/RELAP5/MOD3.1 Code Manual**

## **Volume I: SCDAP/RELAP5 Interface Theory**

**Contributing Authors:**

**C. M. Allison  
G. A. Berna  
E. W. Coryell  
K. L. Davis  
D. T. Hagrman  
J. K. Hohorst  
L. J. Siefken**

**Editor:  
E. W. Coryell**

**October 1993**

**Idaho National Engineering Laboratory  
EG&G Idaho, Inc.  
Idaho Falls, Idaho 83415**

**Prepared for the  
Division of Systems Research  
Office of Nuclear Regulatory Research  
U. S. Nuclear Regulatory Commission  
Washington, D.C. 20555  
Under DOE Contract No. DE-AC07-761D01570  
FIN W6095**



## **ABSTRACT**

The SCDAP/RELAP5 code has been developed for best estimate transient simulation of light water reactor coolant systems during a severe accident. The code models the coupled behavior of the reactor coolant system, core, fission product released during a severe accident transient as well as large and small break loss of coolant accidents, operational transients such as anticipated transient without SCRAM, loss of offsite power, loss of feedwater, and loss of flow. A generic modeling approach is used that permits as much of a particular system to be modeled as necessary. Control system and secondary system components are included to permit modeling of plant controls, turbines, condensers, and secondary feedwater conditioning systems.

This volume describes the organization and manner of the interface between severe accident models which are resident in the SCDAP portion of the code and hydrodynamic models which are resident in the RELAP5 portion of the code. A description of the organization and structure of SCDAP/RELAP5 is presented. Additional information is provided regarding the manner in which models in one portion of the code impact other parts of the code, and models which are dependent on and derive information from other subcodes.



## EXECUTIVE SUMMARY

The specific features of SCDAP/RELAP5/MOD3.1 are described in this five volume set of manuals covering the theory, use, and assessment of the code for severe accident applications. This set replaces the SCDAP/RELAP5/MOD3 Code Manual, NUREG/CR-5273.

The SCDAP/RELAP5 computer code is designed to describe the overall reactor coolant system (RCS) thermal-hydraulic response, core damage progression, and in combination with VICTORIA<sup>a</sup>, fission product release and transport during severe accidents. The code is being developed at the Idaho National Engineering Laboratory (INEL) under the primary sponsorship of the Office of Nuclear Regulatory Research of the U.S. Nuclear Regulatory Commission (NRC).

The code is the result of merging the RELAP5/MOD3<sup>b</sup> and SCDAP models. The RELAP5 models calculate the overall RCS thermal hydraulics, control system interactions, reactor kinetics, and the transport of noncondensable gases. Although previous versions of the code have included the analysis of fission product transport and deposition behavior using models derived from TRAP-MELT, this capability is being replaced through a data link to the detailed fission product code, VICTORIA, as a result of an effort to reduce duplicative model development and assessment.

The SCDAP code models the core behavior during a severe accident. Treatment of the core includes fuel rod heatup, ballooning and rupture, fission product release, rapid oxidation, zircaloy melting, UO<sub>2</sub> dissolution, ZrO<sub>2</sub> breach, flow and freezing of molten fuel and cladding, and debris formation and behavior. The code also models control rod and flow shroud behavior.

The RELAP5 code is based on a nonhomogeneous and nonequilibrium model for the two-phase system that is solved by a fast, partially implicit numerical scheme to permit economical calculation of system transients. The objective of the RELAP5 development effort from the outset was to produce a code that includes important first order effects necessary for accurate prediction of system transients but is sufficiently simple and cost effective such that parametric or sensitivity studies are possible. The development of SCDAP/RELAP5 has this same focus.

The code includes many generic component models from which general systems can be simulated. The component models include fuel rods, control rods, pumps, valves, pipes, heat structures, reactor point kinetics, electric heaters, jet pumps, turbines, separators, accumulators, and control system components. In addition, special process models are included for effects such as form loss, flow at an abrupt area change, branching, choked flow, boron tracking, and noncondensable gas transport.

The development of the current version of the code was started in the spring of 1992. This version contains a number of significant improvements to the SCDAP models since the last versions of the code, SCDAP/RELAP5/MOD2.5 and SCDAP/RELAP5/MOD3[7af], were released. These improvements include the addition of several new models to describe the earlier phases of a severe accident, changes in

---

a. T. Heames et al., *VICTORIA: A Mechanistic Model of Radionuclide Behavior in the Reactor Coolant System Under Severe Accident Conditions*, NUREG/CR-5545, SAND90-0756, Rev. 1, December 1992.

b. C. M. Allison, C. S. Miller, N. L. Wade (Eds.) *RELAP5/MOD3 Code Manual*, Volumes I through IV, NUREG/CR-5535, EGG-2596, June 1990.

the late phase models to provide more “physically intuitive” behavior for full plant calculations, and changes to improve the overall reliability and usability of the code. The improvements in the early phase models include the addition of models to treat (a) the effects of grid spacers including the effects of Inconel spacer grid-zircaloy cladding material interactions, (b) BWR B<sub>4</sub>C control blade-zircaloy channel box material interactions, and (c) accelerated heating, melting, and hydrogen generation during the reflood of damaged fuel rods. An extension to the molten pool models to treat the sporadic growth of the boundaries of the molten pool into adjacent regions of relatively intact assemblies or rubble debris beds is the most significant change to the late phase models. Improvements in overall reliability and usability of the code for plant calculations include changes in the overall code numerics to reduce the likelihood of numerical instabilities or code failures and changes in the codes input/output processors. The most noticeable of these for the code users is the conversion of the SCDAP input to a form more compatible with the RELAP5 style. In addition to these modeling and coding changes, SCDAP/RELAP5/MOD3.1 has also been subjected to (a) an intensive effort of verification testing to identify and resolve outstanding code errors and (b) a systematic assessment of the code to quantify the uncertainties in the predicted results.

This volume, Volume I, describes the organization and manner of interface between severe accident models which are resident in the SCDAP portion of the code and hydrodynamic models resident in RELAP5. It provides the user with an understanding of the overall architecture of the code, and the underlying assumptions and simplifications used to link portions of SCDAP/RELAP5, so an intelligent assessment of the applicability and accuracy of the resulting calculation can be made.

## **ACKNOWLEDGMENTS**

Development of a complex computer code such as SCDAP/RELAP5 is the result of a team effort. Acknowledgments are made to those who made significant contributions to the earlier versions of SCDAP/RELAP5 in particular for the contributions of G. H. Beers, E. R. Carlson, and T. M. Howe. Acknowledgment is also made of E. C. Johnsen for her work in code configuration control, to B. D. Reagan for her support in preparing figures and correcting equations, and to L. G. Price and N. Wade for technical editing support. The authors also acknowledge the RELAP5 development team, specifically R. J. Wagner, R. A. Riemke, and C. S. Miller for their contributions to SCDAP/RELAP5.

The SCDAP/RELAP5 Program is indebted to the technical monitors responsible for directing the overall program: Dr. Y. Chen of the U. S. Nuclear Regulatory Commission and Mr. W. H. Rettig of the Department of Energy Idaho Operations Office. Finally, acknowledgment is made of those many code users who have been very helpful in stimulating correction of code deficiencies with special appreciation to Dr. T. J. Haste and L. Nilsson for the many hours of technical review they provided.



# CONTENTS

ABSTRACT .....	iii
EXECUTIVE SUMMARY .....	v
ACKNOWLEDGMENTS .....	vii
FIGURES .....	xi
TABLES .....	xii
 1. INTRODUCTION .....	 1-1
1.1 General Code Capabilities.....	1-1
1.2 Relationship to Other NRC-Sponsored Software.....	1-2
1.3 Quality Assurance .....	1-2
1.4 Organization of the SCDAP/RELAP5 Manuals.....	1-3
1.5 Organization of Volume I .....	1-3
 2. CODE ARCHITECTURE.....	 2-1
2.1 Computer Adaptability .....	2-1
2.1.1 Source Coding .....	2-1
2.1.2 Systems.....	2-1
2.2 Organization of the Code.....	2-1
2.2.1 Input Processing Overview (INPUTD and RNEWP) .....	2-2
2.2.2 Transient Overview (TRNCTL) .....	2-4
 3. INTERFACE WITH RELAP5 MODELS .....	 3-1
3.1 Common Data.....	3-1
3.2 Variable Exchanges Between SCDAP and RELAP5 .....	3-1
3.3 SCDAP Control of RELAP5 Processes .....	3-5
3.3.1 Reduction of Hydrodynamic Volume Flow Area.....	3-6
3.3.2 Noncondensable Transport.....	3-7
3.4 RELAP5 Control of SCDAP Processes .....	3-7
3.4.1 Component Oxidation Limits.....	3-8
 4. SCDAP/RELAP5 EXTENSIONS TO RELAP5 SYSTEM MODELS.....	 4-1
4.1 Reactor Kinetics Model.....	4-1
4.2 Radiation Model .....	4-2
4.2.1 Radiation Model Governing Equations.....	4-3
4.2.2 View Factors.....	4-9
4.2.3 Mean Path Length .....	4-13
4.2.4 Absorptivities and Emissivities .....	4-14
4.3 Nuclear Heat Model .....	4-17
4.3.1 Fission Product Decay Power.....	4-19
4.3.2 Neutron Capture Correction to Fission Product Decay.....	4-22
4.3.3 Actinide Decay Power.....	4-24
4.3.4 Radial Peaking Factor for Delayed Heat.....	4-25
4.4 Special Techniques .....	4-26

4.4.1	Time Step Control .....	4-26
4.4.2	Radiation Stability Limits .....	4-27
4.4.3	Radiation Time Smoothing.....	4-29
5.	REFERENCES .....	5-1

## FIGURES

Figure 2-1.	SDCAP/RELAP5 architecture with SCDAP specific routines highlighted. ....	2-3
Figure 3-1.	Flow of information from SCDAP to RELAP5.....	3-2
Figure 3-2.	Flow of Information from RELAP5 to SCDAP.....	3-3
Figure 3-3.	Planar blockage model.....	3-7
Figure 3-4.	Model for removal of blockage. ....	3-8
Figure 3-5.	Effect on flow pattern if porous debris melts.....	3-9
Figure 4-6.	Radiation exchange between surfaces and between surfaces and gas. ....	4-3
Figure 4-7.	Radiation exchange between a rod surface and its surroundings. ....	4-5
Figure 4-8.	Geometry for determining view factors between rods.....	4-10
Figure 4-9.	Comparison of decay heat components. ....	4-20
Figure 4-10.	SCDAP/RELAP5 top level organization. ....	4-26

## TABLES

Table 2-1.	Computers executing SCDAP/RELAP5 or RELAP5.....	2-2
Table 4-1.	Water vapor absorption. ....	4-16
Table 4-2.	Energy release from fission of $^{235}\text{U}$ . ....	4-17
Table 4-3.	Decay power correlation constants. ....	4-21
Table 4-4.	G factors for times greater than 10,000 s.....	4-23

# SCDAP/RELAP5/MOD3.1<sup>a</sup> Code Manual

## Volume I: SCDAP/RELAP5 Interface Theory

### 1. INTRODUCTION

The SCDAP/RELAP5 computer code is designed to describe the overall reactor coolant system (RCS) thermal-hydraulic response, core damage progression, and, in combination with VICTORIA,<sup>1</sup> fission product release and transport during severe accidents. The code is being developed at the Idaho National Engineering Laboratory (INEL) under the primary sponsorship of the Office of Nuclear Regulatory Research of the U.S. Nuclear Regulatory Commission (NRC).

#### 1.1 General Code Capabilities

The code is the result of merging the RELAP5/MOD3<sup>2</sup> and SCDAP<sup>3</sup> models. The RELAP5 models calculate the overall RCS thermal hydraulics, control system interactions, reactor kinetics, and transport of noncondensable gases. Although previous versions of the code have included the analysis of fission product transport and deposition behavior using models derived from TRAP-MELT, this capability is being replaced through a data link to the detailed fission product code, VICTORIA, as a result of an effort to reduce duplicative model development and assessment. The SCDAP models calculate the heatup and damage progression in the core structures and the lower head of the reactor vessel. The calculations of damage progression include calculations of the meltdown of fuel rods and structures, the fragmentation of embrittled fuel rods, the formation of a molten pool of core material, and the slumping of molten material to the lower head.

SCDAP/RELAP5 is capable of modeling a wide range of system configurations from single pipes to different experimental facilities to full-scale reactor systems. The configurations can be modeled using an arbitrary number of fluid control volumes and connecting junctions, heat structures, core components, and system components. Flow areas, volumes, and flow resistances can vary with time through either user control or models that describe the changes in geometry associated with damage in the core. System structures can be modeled with RELAP5 heat structures, SCDAP core components, or SCDAP debris models. The RELAP5 heat structures are one-dimensional models with slab, cylindrical, or spherical geometries. The SCDAP core components include representative light water reactor (LWR) fuel rods, silver-indium-cadmium (Ag-In-Cd) and B<sub>4</sub>C control rods and/or blades, electrically heated fuel rod simulators, and general structures. A two-dimensional, finite element model based upon the COUPLE<sup>4</sup> code may be used to calculate the heatup of debris and/or surrounding structures. This model takes into account the decay heat and internal energy of newly fallen or formed debris and then calculates the transport by conduction of this heat in the radial and axial directions to the wall structures and water surrounding the debris. Perhaps the most important use of this model is to calculate the heatup of the vessel wall so that the time at which the vessel may rupture can be determined. Other system components available to the user include pumps, valves, electric heaters, jet pumps, turbines, separators, and

---

a. The MOD3.1 designates a generic version of the code. Where needed, specific developmental version identification will be included with the code name. For example, SCDAP/RELAP5/MOD3[8x] would specify developmental Version 8x.

accumulators. Models to describe selected processes, such as reactor kinetics, control system response, and tracking noncondensable gases, can be invoked through user control.

The development of the current version of the code was started in the spring of 1992. This version contains a number of significant improvements since the last versions of the code, SCDAP/RELAP5/MOD2.5 and SCDAP/RELAP5/MOD3[7af], were released. These improvements include the addition of several new models to describe the earlier phases of a severe accident, changes in the late phase models to provide more “physically intuitive” behavior for full plant calculations, and changes to improve the overall reliability and usability of the code. The improvements in the early phase models include the addition of models to treat (a) the effects of grid spacers including the effects of Inconel spacer grid-zircaloy cladding material interactions, (b) BWR B<sub>4</sub>C control blade-zircaloy channel box material interactions, and (c) accelerated heating, melting, and hydrogen generation during the reflood of damaged fuel rods. An extension to the molten pool models to treat the sporadic growth of the boundaries of the molten pool into adjacent regions of relatively intact assemblies or rubble debris beds is the most significant change to the late phase models. Improvements in overall reliability and usability of the code for plant calculations include changes in the overall code numerics to reduce the likelihood of numerical instabilities or code failures and changes in the codes input/output processors. The most noticeable of these for the code users is the conversion of the SCDAP input to a form more compatible with the RELAP5 style. In addition to these modeling and coding changes, SCDAP/RELAP5/MOD3.1 has also been subjected to (a) an intensive effort of verification testing to identify and resolve outstanding code errors and (b) a systematic assessment of the code to quantify uncertainties in the predicted results.

## 1.2 Relationship to Other NRC-Sponsored Software

SCDAP/RELAP5 and RELAP5 are developed in parallel and share a common configuration. Both codes share a common source deck. Separate codes are formed only prior to compilation, so changes made to the source deck are automatically reflected in both codes.

The development and application of the code is also related to several other NRC-sponsored software packages. Theoretical work associated with the development of PARAGRASS-VFP<sup>5</sup> has resulted in model improvements for fission product release. A data link to the VICTORIA code will allow for the detailed treatment of phenomena such as fission product and aerosol transport, deposition, and resuspension. A link with PATRAN<sup>6</sup> and ABAQUS<sup>7</sup> provides the user with the means to calculate the details of lower head failure. Animated plant response displays are possible through links to the Nuclear Plant Analyzer (NPA)<sup>8</sup> display software, which gives the user an efficient way of analyzing the large amount of data generated. Detailed plant simulations from accident initiation through release of fission products to the atmosphere are made available through links to the CONTAIN<sup>9</sup> containment response and CRAC2<sup>10</sup> or MACCS<sup>11</sup> atmospheric dispersion consequence codes.

## 1.3 Quality Assurance

SCDAP/RELAP5 is maintained under a strict code configuration system that provides a historical record of the changes made to the code. Changes are made using an update processor that allows separate identification of improvements made to each successive version of the code. Modifications and improvements to the coding are reviewed and checked as part of a formal quality program for software. In addition, the theory and implementation of code improvements are validated through assessment

calculations that compare the code-predicted results to idealized test cases or experimental results.

## **1.4 Organization of the SCDAP/RELAP5 Manuals**

The specific features of SCDAP/RELAP5/MOD3.1 are described in a five-volume set of manuals covering the theory (Volume II) user's guidelines and input manual (Volume III), material properties (Volume IV), and assessment (Volume V). Although Volume I describes (a) the overall code architecture, (b) interfaces between the RELAP5 and SCDAP models, and (c) any system models unique to SCDAP/RELAP5, the code user is referred to the companion set of six volumes which describe the RELAP5 system thermal hydraulics and associated models.

Volume I presents a description of SCDAP/RELAP5/MOD3.1-specific thermal-hydraulic models (relative to RELAP5/MOD3), and interfaces between the thermal-hydraulic models and damage progression models.

Volume II contains detailed descriptions of the severe accident models and correlations. It provides the user with the underlying assumptions and simplifications used to generate and implement the basic equations into the code, so an intelligent assessment of the applicability and accuracy of the resulting calculation can be made.

Volume III provides the user's guide and code input for the severe accident modeling. SCDAP input was recently changed to be consistent with the free-form input used by RELAP5. User guidelines are produced specifically for the severe accident code. The user should also refer to the RELAP5/MOD3 Code Manual Volume V: User Guidelines for a complete set of guidelines.

Volume IV describes the material property library, MATPRO. It contains descriptions of the material property subroutines available for severe accident analysis.

Volume V documents the assessments of SCDAP/RELAP5/MOD3.1 performed on versions released since the 1993 deficiency resolution effort. It includes nodalization sensitivity studies and time-step sensitivity studies, assessments using standard PWR and BWR plant models, and assessments using code-to-data comparisons.

## **1.5 Organization of Volume I**

Volume I describes the organization and manner of the interface between severe accident models which are resident in the SCDAP portion of the code and hydrodynamic models which are resident in the RELAP5 portion of the code. Section 2 describes the organization and structure of SCDAP/RELAP5. Section 3 describes the manner in which models in one portion of the code impact other parts of the code. Section 4 describes extensions to RELAP5 models and to its procedure for time step control. Section 5 provides references.



## **2. CODE ARCHITECTURE**

Modeling flexibility, user convenience, computer efficiency, and design for future growth were primary considerations in the development of SCDAP/RELAP5. The following sections describe computer adaptability, code organization, input processing, and transient operation.

### **2.1 Computer Adaptability**

#### **2.1.1 Source Coding**

SCDAP/RELAP5 is written in FORTRAN 77. Compile time-options are provided to allow operation on 64-bit machines and 32-bit machines that have double-precision (64-bit), floating-point arithmetic. A common source is maintained for all computer versions. Reported errors are resolved on all computer versions derived from the common source.

SCDAP/RELAP5 minimizes the need for hardware specific coding through the use of generic functions, character variables and statements, and open statements. The bit handling functions used are from a Mil-spec standard and many computers have implemented that standard. Some machine dependent coding is needed to overcome deficiencies in the Fortran standard. For example, the standard does not allow specification of variable range and precision requirements. Unless modified, the Fortran for a 64-bit machine in single precision would use 64 bits while the 32-bit machine would use only 32 bits. Additional statements are needed to indicate double precision on the 32-bit machine. Some compilers have options for automatically converting to double precision, but that is nonstandard and not available on all systems. Nonstandard coding is needed in some subroutines to define the smallest and largest floating point numbers, the smallest floating point increment, and to access the radix, fraction, and power part of a floating point number. The next standard should remedy these, but until then, precompilers are used to handle hardware and software differences.

#### **2.1.2 Systems**

The SCDAP/RELAP5 computer program should execute on a wide variety of scientific computers with minimal modifications. In particular, the code should execute on all 64-bit computers, that is computers using 64 bits for both floating point and integer arithmetic. It should also execute on the multitude of 32-bit computers that range from workstations to supercomputers and that have 32-bit integer arithmetic but provide 64-bit floating point arithmetic through double precision operations. The code is maintained for all computers in a common source file, and through one or two stages of precompiling, the code is made suitable for a particular computer. Table 2-1 lists the computers where SCDAP/RELAP5 and RELAP5 test problems have been run.

## **2.2 Organization of the Code**

SCDAP/RELAP5 is coded in a modular fashion using top-down structuring. The various models and procedures are isolated in separate subroutines. Figure 2-1 shows an overview of the code architecture.

Input processing is performed in INPUTD and associated subroutines. Transient control is performed

**Table 2-1.** Computers executing SCDAP/RELAP5 or RELAP5.

Computer Identification
Cray X-MP 2/16
DEC Alpha 3000/500X
DEC 5000/200
HP 720
HP 735
HP 750
IBM R6000/320
IBM R6000/370
IBM R6000/540
IBM R6000/Power2/590
SGI Indigo
SGI Crimson
Sun Sparc2
Sun Sparc

by TRNCTL and associated subroutines. The STRIPF routine extracts data from the restart plot file for use in other computer programs. Because of their complexity, the input processing and transient control routines are described in more detail in the Sections 2.2.1 and 2.2.2.

### 2.2.1 Input Processing Overview (INPUTD and RNEWP)

The input processing is performed in three phases. In the first phase, the input data is read and checks are made for typing and punctuation errors (such as multiple decimal points and letters in numerical fields), and stores the data keyed by card number so that the data are easily retrieved. A listing of the input data is provided, and punctuation errors are noted.

During the second phase, restart data from a previous simulation are read if the problem is a RESTART type, and all input data are processed. Some processed input is stored in fixed common blocks, but the majority of the data are stored in dynamic data blocks that are created only if needed by a problem and sized to the particular problem. In a NEW-type problem, dynamic blocks must be created. In RESTART problems, dynamic blocks may be created, deleted, added to, partially deleted, or modified as modeling features and components within models are added, deleted, or modified. Extensive input checking is done, but at this level checking is limited to new data from the cards being processed. Relationships with other data cannot be checked because the latter may not yet be processed. As an illustration of this level of checking, junction data are checked to determine if they are within the appropriate range, such as positive, nonzero, or between zero and one; and volume connection codes are

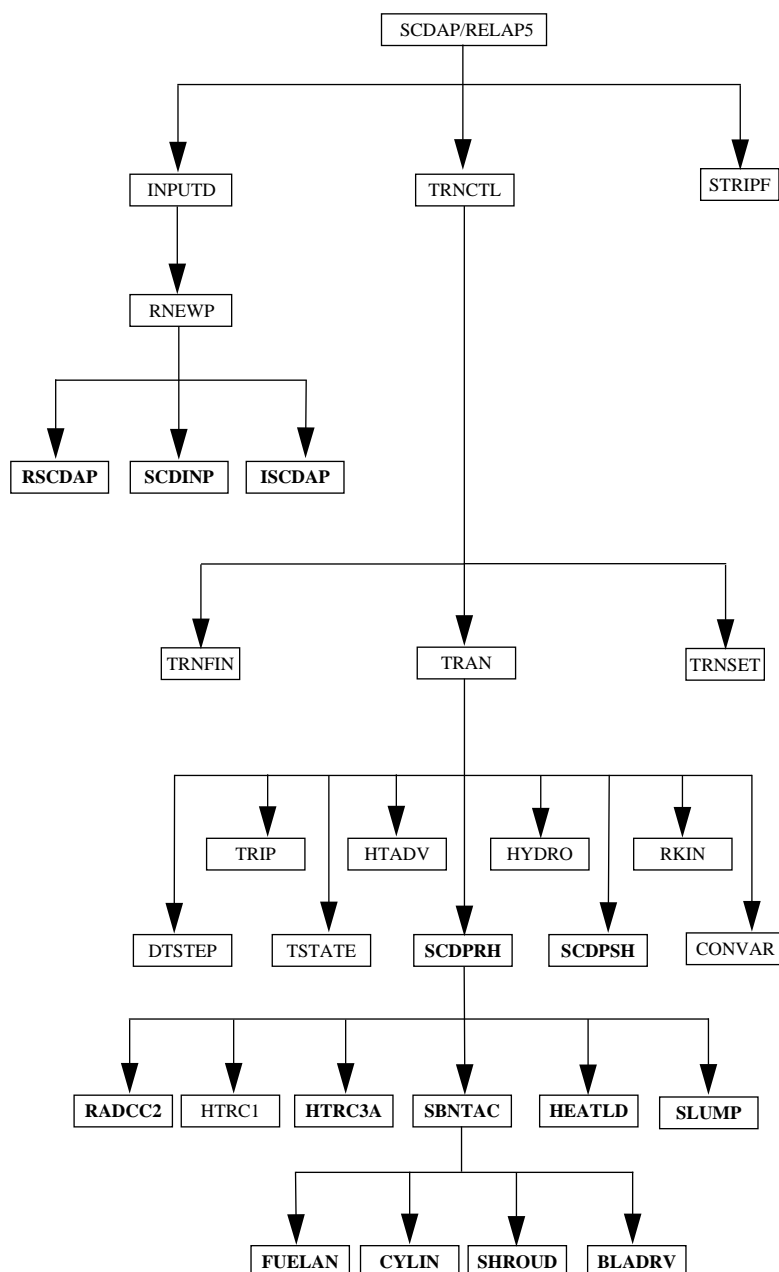


**Figure 2-1.** SCDAP/RELAP5 architecture with SCDAP specific routines highlighted.

checked for proper format. However, no attempt is made at this point to check whether or not referenced volumes exist in the problem until all input data are processed.

The third phase of processing begins after all input data have been processed. Because all data have been placed in common or dynamic data blocks during the second phase, complete checking of interrelationships can proceed. Examples of cross-checking are existence of hydrodynamic volumes

referenced in junctions and heat structure boundary conditions; entry or existence of material property data specified in heat structures; and validity of variables selected for minor edits, plotting, or used in trips and control systems. As the cross-checking proceeds, cross-linking of the data blocks is done so that it need not be repeated at every time step. The initialization required to prepare the model for start of transient advancement is done at this level.

Input data editing and diagnostic messages can be generated during the second and/or third phases. Input processing for most models generates output and diagnostic messages during both phases.

As errors are detected, various recovery procedures are used so that input processing can be continued and a maximum amount of diagnostic information can be furnished. Recovery procedures include supplying default or replacement data, marking the data as erroneous so that other models do not attempt use of the data, or deleting the bad data. The recovery procedures sometimes generate additional diagnostic messages. Often after attempted correction of input, different diagnostic messages appear. These can be due to continued incorrect preparation of data, but the diagnostics may result from the more extensive testing permitted as previous errors are eliminated.

The input processing for the SCDAP portion of the code is performed in three main subroutines as shown in Figure 2-1, RSCDAP, SCDINP, and ISCDAP. These subroutines perform the following functions:

- |        |  |
|--------|--|
| RSCDAP | Processes the new style of input based upon the RELAP5 approach. This is the preferred input option.   |
| SCDINP | Processes the old style input which allows for backward compatibility. However, this routine will gradually be phased out.   |
| ISCDAP | Initializes the SCDAP related variables in the code, maps fuel element locations into thermal-hydraulic volumes, and performs input consistency checks once all input data has been read in. |

## 2.2.2 Transient Overview (TRNCTL)

Subroutine TRNCTL consists only of the logic to call the next lower level routines.

Subroutine TRNSET brings dynamic blocks required for transient execution from disk into computer central memory, performs final cross-linking of information between data blocks, sets up arrays to control the sparse matrix solution, establishes scratch work space, and returns unneeded computer memory. Subroutine TRAN, the driver, controls the transient advancement of the solution. Nearly all the execution time is spent in this subroutine, and TRAN is also the most demanding of memory. The subroutine TRNFIN releases space for the dynamic data blocks that are no longer needed and prints the transient timing summary.

The following description is presented for selected subroutines driven by TRAN (see Figure 2-1):

DTSTEP	Determines the time step size, controls output editing, and determines whether transient advancements should be terminated. During program execution, this module displays such information as CPU time, problem time, and the maximum cladding temperature on a terminal screen.
TRIP	Evaluates logical statements. Each trip statement is a simple logical statement which has a true or false result. The decision of what action is needed resides within the components in other modules. For example, valve components open or close the valve based on trip values; pump components test trip status to determine whether a pump electrical breaker has tripped.
TSTATE	Calculates the thermodynamic state of the fluid in each hydrodynamic user-defined time-dependent volume.
HTADV	Advances heat conduction/transfer solutions using previous-time-step reactor kinetics power and previous-time-step hydrodynamic conditions for computing heat transfer coefficients. It calculates heat transferred across solid boundaries of hydrodynamic volumes.
SCDPRH	Advances the heat conduction, mechanical response (including changes in geometry), and fission gas release models using previous-time-step hydrodynamic conditions. It is in this block that nearly all of the SCDAP core component routines are exercised.
HYDRO	Advances the hydrodynamic solution.
SCDPSH	Drives the COUPLE subcode.
RKIN	Advances the reactor kinetics of the code. It computes the power behavior in a nuclear reactor using the space-independent or point kinetics approximation which assumes that power can be separated into space and time functions.
CONVAR	Provides the capability of simulating control systems typically used in hydrodynamic systems. It consists of several types of control components. Each component defines a control variable as a specific function of time advanced quantities. The time advanced quantities include quantities from hydrodynamic volumes, junctions, pumps, valves, heat structures, reactor kinetics, trip quantities, and the control variables themselves. This permits control variables to be developed from components that perform simple, basic operations.
RADCC2	Calculates the radiation heat transfer in a fuel bundle.
HTRC1	Computes heat transfer coefficients for air-water mixtures, single phase liquids, subcooled nucleate boiling, saturated nucleate boiling, subcooled transition film boiling, saturated transition film boiling, subcooled film boiling, saturated film boiling, and single phase vapor convection.
HTRC3A	Calculates heat transfer from debris to coolant.
SBNTAC	Drives all SCDAP components.
HEATLD	Calculates the heatup of circulating liquefied debris contained by hardpan. The subroutine also calculates the thickness of the hardpan and spreading of the molten pool.

- SLUMP     Determines whether a new unique slumping of core material into lower vessel region occurred during a time step. If slumping occurred, it calculates the total mass of material that will end up eventually falling into the lower vessel region due to this slumping. This falling may be spread out over many time steps.
- FUELAN    Calculates response of LWR fuel rod component.
- CYLIN     Calculates response of LWR control rod component.
- SHROUD    Calculates response of shroud component.
- BLADRV    Calculates response of the control blade/channel box component.

Although there is a conceptual boundary between the hydrodynamic and severe core damage subroutines of the SCDAP/RELAP5 code, each is intimately bound to the other and information is freely exchanged across the conceptual boundary.

The top-level organization of SCDAP/RELAP5 has been significantly changed. Previous versions advanced the hydrodynamic calculation, determined whether the time step needed repetition, and then proceeded to the severe accident advancement. This effectively forced the SCDAP subroutines to accept the hydrodynamic advancement, and prevented the repetition of a time step due to conditions within the severe accident block. The current organization allows advancement of the severe accident block within the hydrodynamic calculation, and allows the severe accident block to have significantly greater control of the decision as to whether a specified set of conditions are acceptable, thereby influencing the time step control.

### 3. INTERFACE WITH RELAP5 MODELS

This section describes the interface of SCDAP and its models for severe core damage with RELAP5 and its models for thermal hydraulic behavior. The exchange of information between these two parts of the code are also summarized.

#### 3.1 Common Data

The exchanges of information between SCDAP and RELAP5 occur through the medium of common blocks. The RELAP5 common blocks named /voldat/ and /jundat/ contain the variables that are used and modified by SCDAP. These RELAP5 variables are used and modified in several different subroutines in SCDAP. The SCDAP subroutine named SCDPRH is called by the RELAP5 subroutine named TRAN to account for the behavior of SCDAP heat structures on the behavior of the fluid in the region of the reactor core and lower head of the reactor vessel.

#### 3.2 Variable Exchanges Between SCDAP and RELAP5

This section describes the flow of information between the SCDAP and RELAP5 parts of the SCDAP/RELAP5 code. This flow of information occurs at every time step and results in an active link of the SCDAP models with the RELAP5 models. The variables in the flow of information that are calculated in SCDAP and then passed on to RELAP5 are listed and a description is given of the impact on the RELAP5 calculations of these variables received from SCDAP. Then, the variables that are calculated in RELAP5 and passed on to SCDAP are listed and a description is given of the impact on the SCDAP calculations of the variables received from RELAP5. A summary of the flow of information from SCDAP to RELAP5 is shown in Figure 3-1. This figure identifies each subroutine in SCDAP that supplies information to RELAP5 and each subroutine in RELAP5 that applies the information received from SCDAP. The names of the variables that contain the transmitted information are also shown. The flow of information from RELAP5 to SCDAP is shown in Figure 3-2.

The variables calculated by SCDAP and passed on to RELAP5 are: (1) surface temperatures of intact SCDAP heat structures and COUPLE heat structures, (2) heat transferred to fluid by radiation from intact heat structures, (3) changes in flow area and hydraulic diameter, (4) rate of consumption of steam and the corresponding production of hydrogen, (5) release of fission gases such as Xe and Kr, and (6) heat transferred from porous debris to fluid in contact with the porous debris, heat transferred from a molten pool to fluid, and heat transferred from slumping core material to fluid. These variables and their impact on RELAP5 calculations are described next.

The surface temperatures of SCDAP and COUPLE heat structures are passed on to RELAP5 in order to calculate the convective heat transfer at the surface of the heat structures. These variables are named  $tcond3(is,j,k)$  and  $tz(js)$ , where "is" is the radial node at the surface of the SCDAP heat structures, "j" is the axial node number, "k" is the core component identification number, and "js" is a COUPLE heat structure node number that is located at the surface. These variables impact the calculated temperature and vapor generation rate for the fluid that interfaces with SCDAP and COUPLE heat structures. The surface temperatures of SCDAP heat structures are calculated in the SCDAP heat conduction model, which is programmed in a subroutine named HEATC2. The surface temperatures are calculated for each axial node

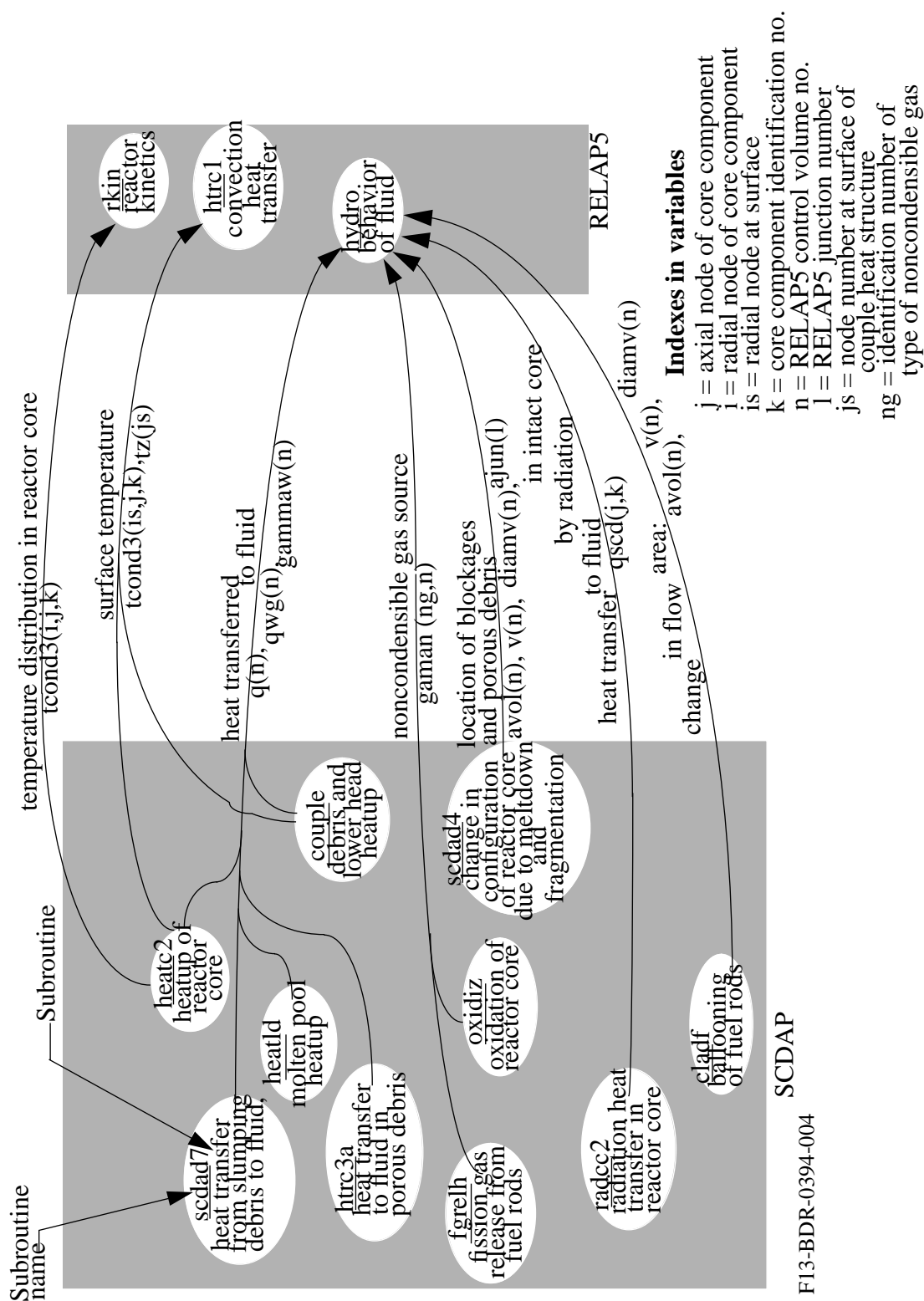


**Figure 3-1.** Flow of information from SCDAP to RELAP5.

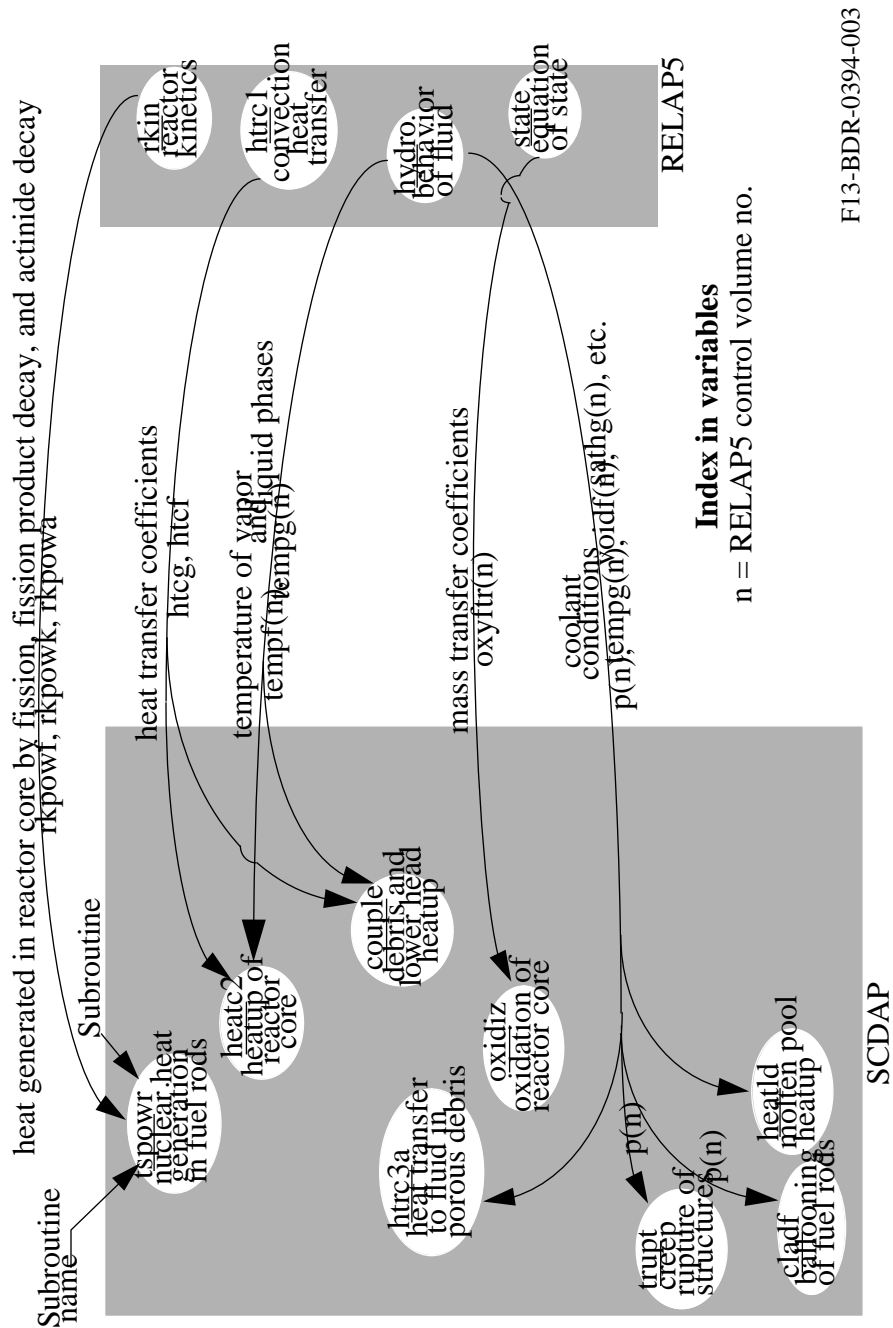


**Figure 3-2.** Flow of Information from RELAP5 to SCDAP.

of each component of the reactor core. The surface temperatures of the COUPLE heat structures are calculated in the subroutine named GELB. The surface temperatures for each COUPLE node that interfaces with fluid are passed on to RELAP5. The surface temperatures are used by the RELAP5

subroutine named HTRC1 to calculate for each heat structure the convective heat transfer between the surfaces of the heat structure and the liquid and vapor phases of the fluid interfacing with the heat structure. The volumetric generation rate of vapor at the surface of each heat structure and the heat transfer coefficient to the vapor and liquid phases of water are also calculated by subroutine HTRC1.

The heat transferred by radiation from the surfaces of SCDAP and COUPLE heat structures to the fluid interfacing with these heat structures is calculated by SCDAP and passed on to RELAP5 in order to be included in calculation of the internal energy and temperature of the fluid interfacing with these structures. The radiation heat transfer from the SCDAP heat structures to the interfacing fluid is calculated in the subroutine named RADCC2. The radiation heat transfer is stored in the variable named  $qscd(j,k)$ , where the index “j” is the axial node number, and the index “k” is the component number. The variable  $qscd$  also stores the convective heat transfer. This variable is also updated in subroutine SCDAD4 to account for heat transferred to the fluid by gamma radiation from SCDAP heat structures.

The degradation of the reactor core has a significant impact on the flow of coolant through the region of the reactor core and the region of the lower head. The ballooning of fuel rods may result in the flow area at the location of the ballooned fuel rods being reduced by more than 50%. The metallic meltdown of fuel rods may result in a 100% blockage to flow in the axial direction at the locations where the slumping material solidifies. The fragmentation of embrittled fuel rods that quench may result in a factor of one hundred increase in the flow resistance at the locations with fragmented fuel rods. The melting of ceramic material may result in a 100% blockage to flow in the axial and lateral directions. The remelting and slumping of blockages results in the resumption of flow at locations where it previously did not occur due to the blockages. The flow areas, volumes, volume lengths, and hydraulic diameters of RELAP5 control volumes in the core region and lower head are adjusted by SCDAP to account for the changes in geometry caused by fuel rod ballooning, fuel rod and control rod meltdown, fragmentation of embrittled fuel rods, and slumping of core material to the lower head of the reactor vessel. The RELAP5 variables updated by SCDAP are: (1)  $ajun(l)$ , which are the junction areas, (2)  $avol(n)$ , which are the control volume areas, (3)  $v(n)$ , which are the volumes of control volumes, (4)  $dl(n)$ , which are the lengths of control volumes, and (5)  $diamv(n)$ , which are the hydraulic diameters of control volumes. The index “l” refers to the junction index and the index “n” refers to the volume index. The junction areas in both the axial and lateral directions are adjusted. These RELAP5 variables are adjusted in subroutine SCDAD4 to account for degradation of the reactor core and are adjusted in subroutine SCDAD7 to account for the filling of the lower head with slumping material from the core region.

The RELAP5 variable that stores for each control volume the source term of noncondensable gases is adjusted by SCDAP to account for the production of hydrogen by the oxidation of the reactor core and to account for the release of noncondensable fission gases from fuel rods. The RELAP5 variable updated by SCDAP is  $gaman(ng,n)$ , which is the volumetric source term for the ng-th type of noncondensable gas for the control volume with the index “n”. This variable is updated in subroutines OXIDIZ (fuel rod oxidation), OXDCON (PWR control rod oxidation), BWHTCN (BWR control blade oxidation), BLADRV (BWR control blade oxidation), and FGRELG (fission gas release and fill gas from fuel rods). The source terms for several types of gases are calculated by SCDAP and passed on to RELAP5. The most important noncondensable gas is hydrogen. Other noncondensable gases are Xe, Kr, and He, which is a fill gas for fuel rods. These source terms are updated by SCDAP at each time step for each axial node of each core component.

SCDAP updates three RELAP5 variables to account for the heat transferred from porous debris to fluid, the heat transferred from the outer surface of a molten pool to the fluid in contact with the molten pool, and the heat transferred from slumping debris that breaks up. The variables updated by SCDAP are  $q(n)$ ,  $qwg(n)$ , and  $gammaw(n)$ , where  $q(n)$  is the total heat transferred to the fluid in the RELAP5 control volume with the index “n”,  $qwg(n)$  is the heat transferred to the vapor in this control volume, and  $gammaw(n)$  is the volumetric vapor generation rate in this control volume. These variables are updated in subroutine HTRC3A to account for the heat transferred from porous debris to the fluid in the porous debris. These variables are updated in subroutine SCDPRH to account for the heat transferred from the surfaces of intact SCDAP heat structures and the heat transferred from the surfaces of a molten pool to the fluid in contact with the molten pool. These variables are also updated in subroutine SCDPRH to account for the heat transferred from slumping material to the fluid in contact with the slumping material.

RELAP5 calculates several variables that are transferred to SCDAP to calculate the behavior of the reactor core. The first variable transferred to SCDAP is the power of the reactor core. This variable has three parts; namely  $rkpowf(i)$ , which is the power due to fission,  $rkpowk(i)$ , which is the power due to fission product decay, and  $rkpowa(i)$ , which is the power due to actinide decay. The index “i” is defined by the file manager for RELAP5. The SCDAP subroutine named TSPOWR uses the RELAP5 calculated power to calculate the power in each SCDAP heat structure. The second set of variables transferred to SCDAP from RELAP5 defines fluid conditions for calculating convective heat transfer. The first variable in this set is the heat transfer coefficient to the vapor phase which is named  $htcg$ . The second variable is the heat transfer coefficient to the liquid phase, which is named  $htcf$ . These variables are calculated by the RELAP5 subroutine named HTRC1. The third and fourth variables are the temperatures of the liquid and vapor phases of water. These variables are named  $tempf(n)$  and  $tempg(n)$ , respectively. These temperatures are calculated by the RELAP5 subroutine named HYDRO. These four variables are transferred for each axial node of each SCDAP heat structure and for the nodes at the surface of each COUPLE heat structure. The heat transfer coefficients and fluid temperatures are used to define a boundary condition in SCDAP and COUPLE heat conduction models. The third variable transferred to SCDAP is the rate of mass transfer of steam through the boundary layer at the surface of SCDAP heat structures that are oxidizing. This variable is named  $oxyftr(n)$ , where the index “n” is the number of the RELAP5 control volume. This variable is transferred for each axial node of each SCDAP heat structure. The variable is used to define a boundary condition in the oxidation models. Next, a set of variables are transferred to SCDAP. These variables are: (1) temperature of vapor and liquid phases of water [ $tempf(n)$  and  $tempg(n)$ ], (2) volume fraction of liquid [ $voidf(n)$ ], (3) vapor specific enthalpy [ $sathg(n)$ ] and liquid specific enthalpy [ $sathf(n)$ ] and other thermodynamic and transport properties of the fluid, and (4) saturation temperature [ $satt(n)$ ]. These variables are used by SCDAP to calculate the heat transfer from porous debris to fluid, heat transfer from a molten pool to fluid, and heat transfer from slumping material to fluid. The next variable transferred to SCDAP is the fluid pressure [ $p(n)$ ]. This variable is used by SCDAP to define a boundary condition in the fuel rod ballooning model and to define a boundary condition in the model for creep rupture of the lower head and other structures.

### 3.3 SCDAP Control of RELAP5 Processes

A number of SCDAP phenomena have an impact on RELAP5 processes. These phenomena are described in the following section.

### 3.3.1 Reduction of Hydrodynamic Volume Flow Area

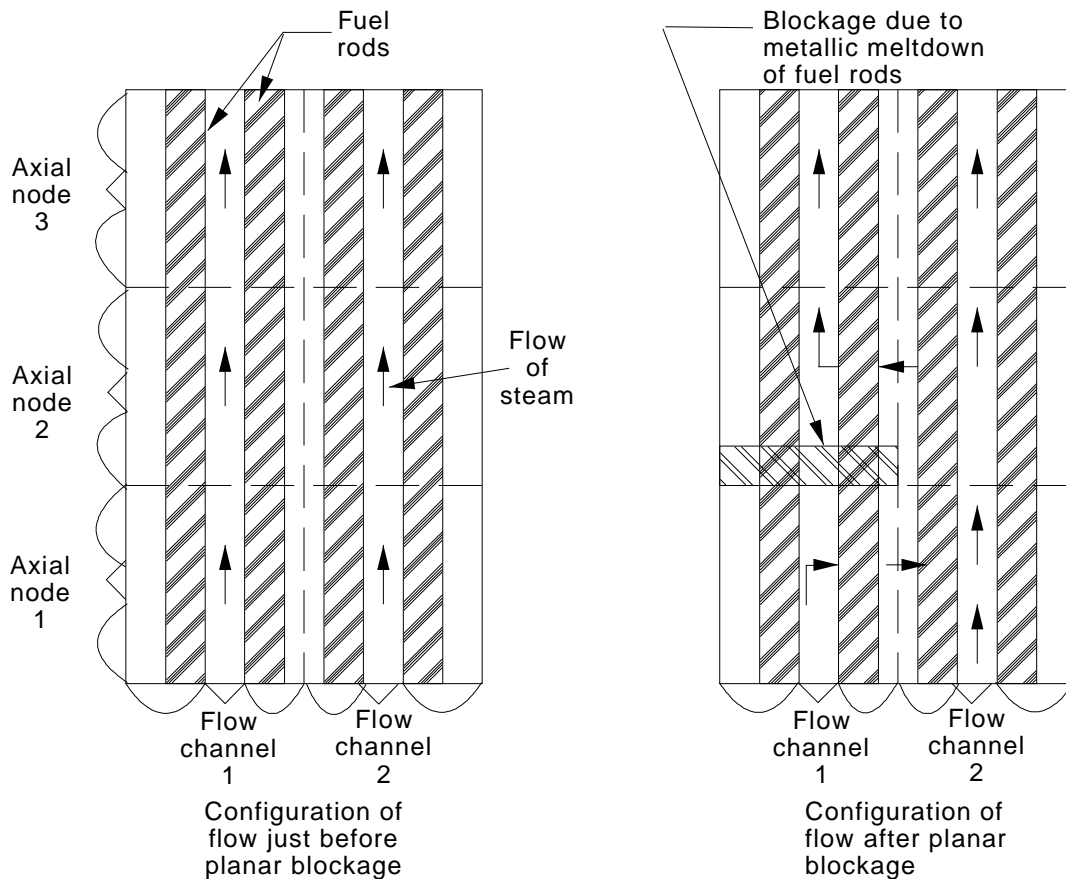
Two potential phenomena can cause a change in the hydrodynamic flow area used by RELAP5. These phenomena are core component ballooning, which would occur in a fuel rod during high temperature accidents, and corium meltdown/relocation, which would occur when a material from a control or fuel rod melts and relocates lower in the core region, creating a planar blockage. These two phenomena are modeled with two different methods.

The reduction of hydrodynamic volume flow area caused by cladding ballooning is accomplished by reducing the value of the variable in which flow area is stored. Because this is a permanent change, unlike flow blockage where the blockage can remelt and move lower, no additional information regarding the flow area prior to flow blockage is required. This reduction in flow area impacts flow in both the axial and cross flow directions.

The model for plane blockage is shown in Figure 3-3. The figure shows the part of a reactor core represented by two flow channels and three axial nodes. The left part of the figure shows the state of the core prior to a blockage, and the right part shows the state after a blockage. The blockage occurs in flow channel 1 of axial node 2 and is caused by the slumping of a liquefied mixture of cladding and dissolved fuel. Because only a small amount of material slumps and the slumping material usually freezes at the location of a grid spacer, the blockage is spread across the flow channel but is small in height. The blockage is planar; it blocks flow in the axial direction at the bottom of axial node 2 of flow channel 1, but only partially blocks flow in the lateral direction at axial node 2 of flow channel 1. It does not block flow in the axial direction at the top part of axial node 1.

A model also removes blockages at locations at which material has slumped away. The model removes both planar blockages (Figure 3-3) and bulk blockages (Figure 3-4). In the case of removing the planar blockage, the model changes the junction flow area at the location of the blockage from zero to the flow area of the junction prior to the blockage. When removing a bulk blockage, the model restores all of the junction flow areas and activates the RELAP5 control volume that models the fluid at that location. Thus, after the removal of the bulk blockage at a location, a calculation is again made of the amount and composition of the fluid at that location and of the thermodynamic state of the fluid.

The blockage model also modifies the flow areas and volumes at locations to account for the compaction that takes place when porous debris melts. The change in configuration represented by the modeling is shown in Figure 3-5. The left part of the figure shows porous debris that is beginning to melt at axial nodes 2 and 3 of flow channel 1. Steam is flowing through both of these axial nodes. The right part of the figure shows the pattern of steam flow after the porous debris at the two axial nodes has completely melted. The melting porous debris at axial node 3 slumps into the open porosity at axial node 2. This compaction results in an open space at axial node 3 and a blockage of steam at axial node 2. To represent this change in configuration, the blockage model assigns a flow area of zero to all of the RELAP5 junctions connected with axial node 2 and deactivates the RELAP5 control volume representing the fluid at axial node 2. For axial node 3, the model assigns the RELAP5 control volume for this location a volume that represents the increase in space resulting from the material at this location slumping to axial node 2.



M158-BDR-1092-008

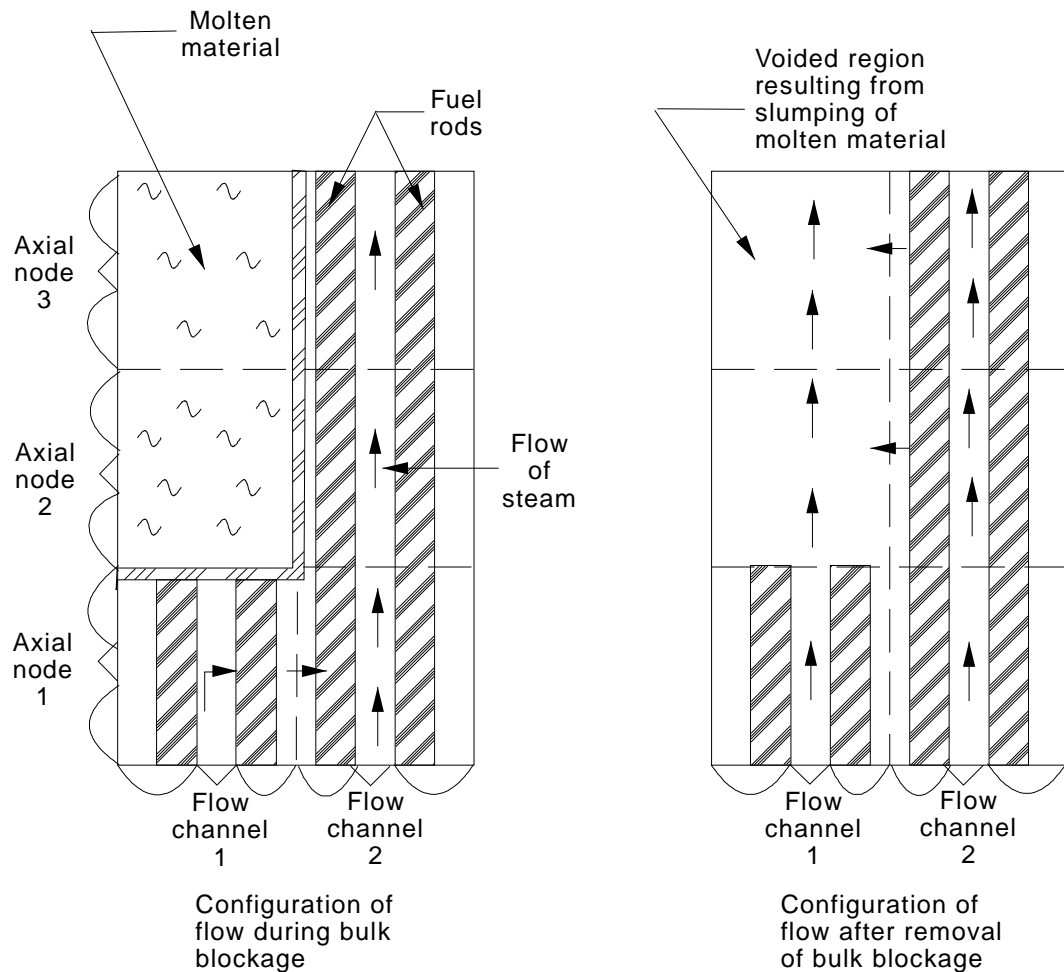
**Figure 3-3.** Planar blockage model.

### 3.3.2 Noncondensable Transport

The SCDAP portion of the code has the capability of releasing noncondensable gases (hydrogen and fission products). The RELAP5 portion of the code must track the migration of these gases through the primary coolant system, and evaluate their impact on the thermal response of the remainder of the system. As a minimum therefore the code user must specify at least hydrogen as a noncondensable on input, in order to force RELAP5 to allocate storage for noncondensable. As documented in Volume IV of Reference 2, the effects of a noncondensable within RELAP5 are represented by multipliers that modify the volumetric heat transfer coefficients. In sufficient quantities the presence of a noncondensable may also impact flow regime determination.

## 3.4 RELAP5 Control of SCDAP Processes

Although most of the information exchange between the hydrodynamic subcode, RELAP5, and the severe accident subcode, SCDAP, involves SCDAP control of RELAP5 processes, one significant SCDAP



M158-BDR-1092-009

**Figure 3-4.** Model for removal of blockage.

model, the core component oxidation model, accepts limits from RELAP5.

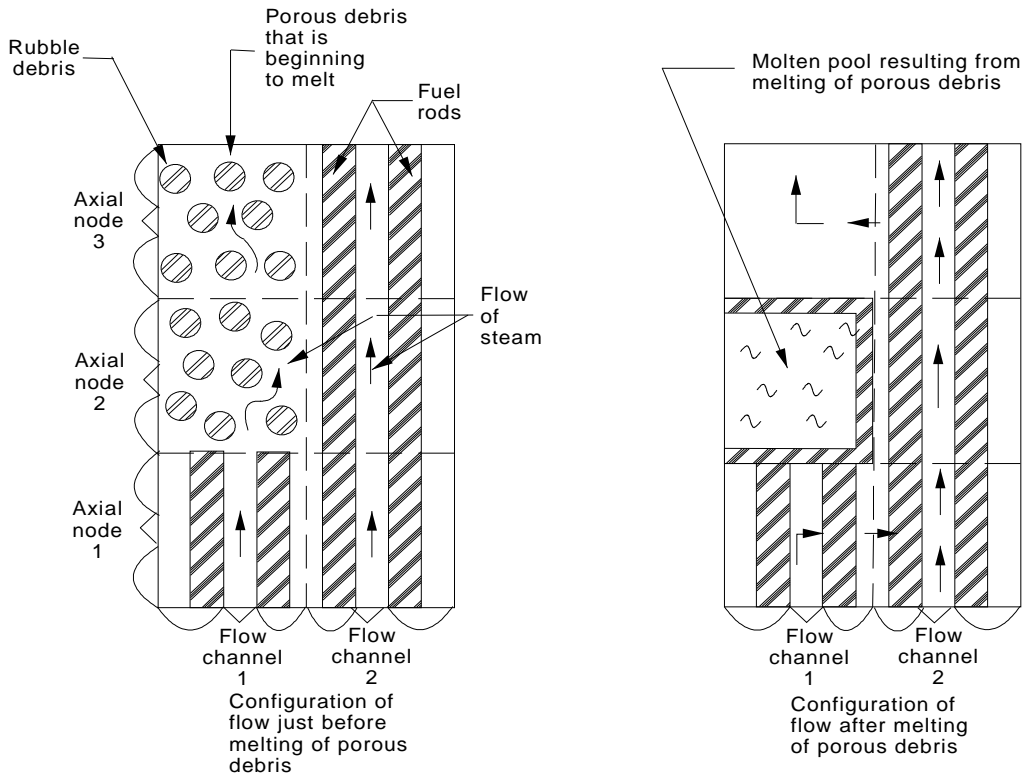
### 3.4.1 Component Oxidation Limits

As described in Volume II of this report, the process of material oxidation within SCDAP/RELAP5 is subjected to three limits.

- The oxidation is terminated when the material is fully oxidized
- The oxidation rate is limited by the availability of steam
- The oxidation rate is limited by the diffusion of water vapor.

The latter two limits are those limits imposed on the SCDAP oxidation process by RELAP5.

The mass of steam within the hydrodynamic volumes adjoining the core component is passed to SCDAP via common block. The oxidation of each component is then calculated starting at the upstream axial node, that is the bottom axial node during upward flow and the top axial node during downward flow.



M158-BDR-1092-011

**Figure 3-5.** Effect on flow pattern if porous debris melts.

The consumption of steam by the oxidation process is then modeled, and the amount of remaining steam is returned to RELAP5 to be moved along during the next time step.

The limitation on the oxidation rate by the diffusion rate of water vapor through the mixture of noncondensable is also imposed on the SCDAP oxidation process by RELAP5. Although this model is documented in detail in Volume II of this report, the limit is calculated by RELAP5 for each volume of the system for each time step, and passed via common block to the SCDAP oxidation routines.



## 4. SCDAP/RELAP5 EXTENSIONS TO RELAP5 SYSTEM MODELS

This section describes extensions to existing RELAP5 models to transform them into SCDAP/RELAP5 specific models.

### 4.1 Reactor Kinetics Model

The RELAP5 reactor kinetics model is extended to SCDAP/RELAP5 by allowing SCDAP component temperatures to impact the temperature feedback, and allowing the resultant power in SCDAP components.

One of two models can be selected for reactivity feedback. One model assumes nonlinear feedback effects from moderator density and fuel temperature changes and linear feedback from moderator temperature changes. It is called the separable model because each effect is assumed to be independent of the other effects. Boron feedback is not provided, but a user-defined boron feedback can be implemented with the control system. The separable model can be used if boron changes are quite small and the reactor is near critical about only one state point.

The separable model defines reactivity as

$$\begin{aligned} r(t) = & r_0 - r_B + \sum_i^{n_s} r_{si}(t) + \sum_i^{n_c} V_{ci} + \sum_i^{n_p} \{ W_{\rho i} R_p [\rho_i(t)] + a_{wi} T_{wi}(t) \} \\ & + \sum_i^{n_F} \{ W_{Fi} R_F [T_{Fi}(t)] + a_{Fi} T_{Fi}(t) \}. \end{aligned} \quad (4-1)$$

The quantity  $r_0$  is an input quantity that represents the reactivity corresponding to assumed steady-state reactor power at  $t=0$ . The quantity  $r_B$  is the bias reactivity, which is calculated during input processing such that  $r(0) = r_0$ . The quantities  $r_{si}$  are obtained from input tables defining  $n_s$  reactivity curves as a function of time. The quantities  $V_{ci}$  and  $n_c$  are control variables that can be user-defined as reactivity contributions.  $R_p$  is a table defining reactivity as a function of the current density of water  $\rho_i(t)$  in the hydrodynamic volume  $i$ ;  $W_{\rho i}$  is the density weighting factor for volume  $i$ ;  $T_{wi}$  is the spatial density averaged temperature of volume  $i$ ;  $a_{wi}$  is the temperature coefficient (not including density changes) for volume  $i$ ; and  $n_p$  is the number of hydrodynamic volumes in the reactor core. The value  $R_F$  is a table defining reactivity as a function of the average fuel temperature  $T_{Fi}$  in a SCDAP fuel rod component;  $W_{Fi}$  and  $a_{Fi}$  are the fuel temperature weighting factor and the fuel temperature coefficient, respectively; and  $n_F$  is the number of SCDAP fuel rod components in the reactor core.

As previously mentioned this model is applicable if the reactor is near critical about only one state point. However, a postulated BWR anticipated transient without scram (ATWS) accident is an example where the reactor could be nearly critical for two different state points. One point is at normal power operating conditions-high moderator and fuel temperatures, highly voided, and no boron. During accident

recovery, the reactor might approach a critical condition with relatively cold moderator and fuel temperatures, with no voids, but with some boron concentration. The reactivity could be nearly critical for both states, but the contributions from the different feedback effects are vastly different. The assumptions of no interactions among the different feedback mechanisms, especially boron, cannot be justified. In this case the tabular model would be more applicable.

The tabular model defines reactivity as

$$r(t) = r_0 - r_B + \sum_i^{n_s} \sigma_{si} + \sum_i^{n_c} V_{ci} + R[\rho(t), T_w(t), T_F(t), B(t)] \quad (4-2)$$

$$\rho(t) = \sum_i^{n_p} W_{\rho i} \rho_i(t) \quad (4-3)$$

$$T_w(t) = \sum_i^{n_p} W_{\rho i} T_{wi}(t) \quad (4-4)$$

$$B(t) = \sum_i^{n_p} W_{\rho i} B_i(t) \quad (4-5)$$

$$T_F(t) = \sum_i^{n_F} W_{Fi} T_{Fi}(t) \quad (4-6)$$

where B is boron density. The average quantities are obtained with the use of one weighting factor for each hydrodynamic volume and each SCDAP component contributing to reactivity feedback. The reactivity function R is defined by a table input by the user. In the TABLE4 option the table is four-dimensional; the TABLE3 option assumes no boron dependence and the table is then three-dimensional. Although the tabular model overcomes the objections of the separable model, because all feedback mechanisms can be non-linear and interactions among the mechanisms are included, the penalty for the expanded modeling capability greatly increases the input data requirements.

## 4.2 Radiation Model

This section describes the radiation heat transfer model used for a LWR core. The radiation model analyzes the radiation exchange between the various components in the core, including the coolant. The model calculates the radiation heat flux absorbed by the coolant and the radiant heat exchange between the surfaces of any vessel component (fuel rod, control rod, or shroud). The radiant heat exchange is a thermal boundary condition used in severe accident analysis of fuel rods, control rods, and flow shrouds.

#### 4.2.1 Radiation Model Governing Equations

A mechanistic radiative heat transfer formulation, which accounts for each surface, the vapor, and each droplet, is complex. To develop such a detailed model for SCDAP/RELAP5 would not be cost effective. Instead, simplified models are used without unduly sacrificing the accuracy of the results.

The radiation model presented here is similar to those developed earlier<sup>12,13,14,15,16,17,18,19</sup> for nuclear reactor applications. The solution method used is the net radiation method for an enclosure. Each component (fuel rod, control rod, or shroud) surface forms one side of an enclosure with  $n$  sides, and the enclosure is filled with coolant (see Figure 4-6). The radiation heat transfer equation for each surface describes radiation exchange with all the surfaces (including itself if it radiates to itself) and absorption and emittance by the enclosed coolant. The  $n$  equations are solved simultaneously by a matrix inversion method to obtain the radiosity (the sum of emitted and reflected radiation energy rates) of each surface. The difference between the radiosity and incident energy from the surroundings gives the net heat flux to or from a surface. The algebraic sum of net heat flux corresponding to each surface gives the total radiation heat absorbed by the coolant.

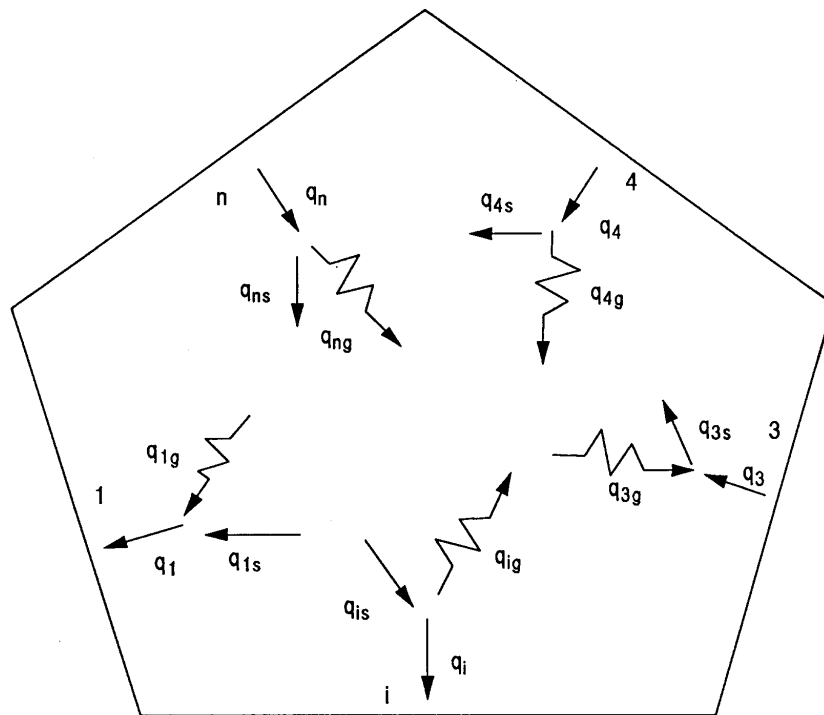


**Figure 4-6.** Radiation exchange between surfaces and between surfaces and gas.

To derive the governing equation of radiation heat exchange for a surface, the following assumptions were made:

- All surfaces are gray, that is, the absorption is independent of wavelength
- All surfaces are diffuse for emission and the isotropic portion of the reflected radiant energy
- Each surface has a uniform temperature and emits radiation uniformly
- Of the reflected radiation from a surface  $i$ , a fraction  $(1 - \mu_i)$  is reflected isotropically (diffuse uniformly in all the directions); and the rest,  $\mu_i$ , is reflected back toward the origin of the incident radiation
- The coolant absorbs and emits radiation
- The coolant is assumed to be steam only with no entrained droplets.

Figure 4-7 shows the radiation exchange mechanism for any surface  $i$ .  $I_i$  is the rate of radiant flux incoming from the surroundings (other surfaces, gas, and possibly surface  $i$ ). A portion,  $a_i$ , of  $I_i$  is absorbed by the surface  $i$ , and the remaining  $(1 - a_i)$  is reflected to the surroundings. The surface  $i$  also emits radiation. Thus, the outgoing radiation energy flux rate (radiosity),  $E_i$ , from a surface  $i$  is composed of emitted and reflected radiation. This gives

$$\begin{aligned}
 E_i &= \epsilon_i \sigma T_i^4 + \rho_i I_i \\
 &= \epsilon_i \sigma T_i^4 + (1 - \epsilon_i) I_i
 \end{aligned} \tag{4-7}$$

where

- $E_i$  = rate of radiant energy outgoing (radiosity) from a unit area of surface  $i$  ( $\text{W/m}^2$ )
- $\epsilon_i$  = the emissivity of surface  $i$  (equal to  $a_i$  for a gray diffuse surface)
- $\sigma$  = Stefan-Boltzmann constant ( $5.668 \times 10^{-8} \text{ W/m}^2 \cdot \text{K}^4$ )
- $T_i$  = the temperature of surface  $i$  (K)
- $\rho_i$  = the reflectivity of surface  $i$  equals  $(1 - a_i) = (1 - \epsilon_i)$
- $I_i$  = the rate of radiant energy incident upon a unit area of surface  $i$  ( $\text{W/m}^2$ ).

Here a relation,  $\rho_i = (1 - a_i) = (1 - \epsilon_i)$ , has been used for an opaque gray surface. The incoming flux,  $I_i$ , is the sum of the portions of the energy leaving all the surfaces of the enclosure that arrives at the  $i^{\text{th}}$  surface. The reflected radiation from a surface will mainly leave the surface in a direction that forms an equal but opposite angle with the surface normal to the direction of the incident radiation, whereas the emitted radiation leaves in all the directions. Therefore, for large or curved surfaces, generally the radiation is reflected backward toward the origin of the incident radiation. Hence, it is assumed<sup>17,18</sup> that a fraction,  $\mu$ , of the incident reflection is reflected backward and the remaining radiation  $(1 - \mu)$  is

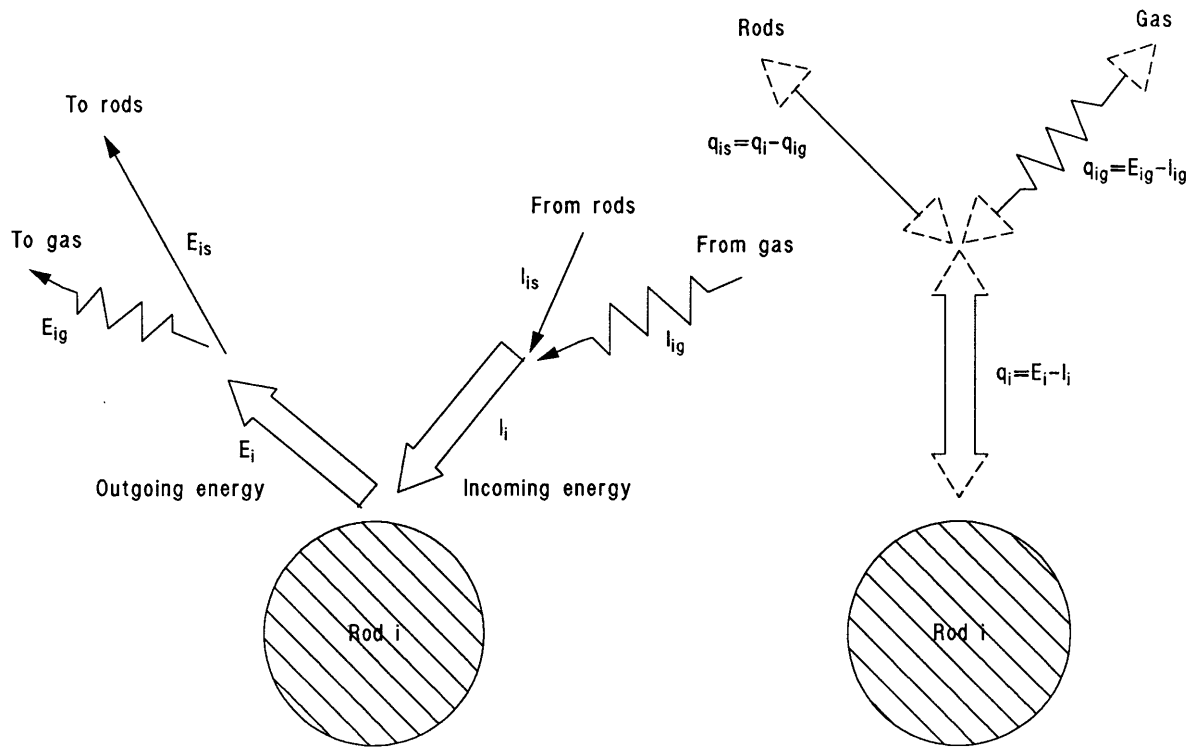


**Figure 4-7.** Radiation exchange between a rod surface and its surroundings.

reflected uniformly in all the directions.

The isotropic part of the outgoing radiation (radiosity),  $E_i^A$ , from a surface  $i$  is given by

$$E_i = \varepsilon_i \sigma T_i^4 + (1 - \mu_i) (1 - \varepsilon_i) I_i \quad (4-8)$$

and the anisotropic part, which is reflected back to the  $j$ -th surface,  $E_{ij}^A$ , is given by

$$E_{ij}^A = \mu_i (1 - \varepsilon_i) I_i \quad (4-9)$$

or

$$\sum_{j=1}^n I_{ij} = \frac{1}{\mu_i (1 - \varepsilon_i)} \sum_{j=1}^n E_{ij}^A. \quad (4-10)$$

The total incoming radiation onto surface  $i$  is the sum of incoming radiation from all the directions,  $I_{ij}$ , including itself:

$$I_i = \sum_{j=1}^n I_{ij} . \quad (4-11)$$

Combining Equations (4-8), (4-10), and (4-11), the following equation is obtained:

$$E_i = \epsilon_i \sigma T_i^4 + \frac{(1 - \mu_i)}{\mu_i} \sum_{j=1}^n E_{ij}^A . \quad (4-12)$$

The incident radiation from the j-th surface reaching the i-th surface consists of the following parts:

- Isotropic part of the radiosity of the j-th surface multiplied by the view factor from surface j to surface i
- The anisotropic part of the radiation emitted in the direction of i-th surface; the total radiosity, sum of (1) and (2), is reduced by the transmissivity of the coolant
- Radiation emitted by the coolant itself.

Therefore,

$$A_i I_{ij} = (E_j^A A_j F_{ji} + E_{ji}^A A_j) \tau_{ji} + \epsilon_{gji} \sigma T_g^4 A_j F_{ji} \quad (4-13)$$

where

$$\begin{aligned} A_i &= \text{the area of surface } i \text{ (m}^2\text{)} \\ F_{ji} &= \text{the view factor of surface } j \text{ to surface } i \\ \tau_{ji} &= \text{the transmissivity of coolant from surface } j \text{ to surface } i = e^{(-K_{gji} L_{ji})} \\ \epsilon_{gji} &= (1 - \tau_{ji}) . \end{aligned}$$

Here  $L_{ji}$  is the mean path (beam) length between surfaces i and j.  $K_{gji}$  is the absorption coefficient (absorptivity per unit length) for the vapor medium and has the units of  $m^{-1}$ . Because liquid droplets are assumed to be absent in the path between i and j, the absorption coefficient for liquid  $K_{lji}$  is taken as zero.

Therefore,  $\tau_{ji}$  and  $\epsilon_{gji}$  are equal to  $e^{-K_{gji} L_{ji}}$  and  $(1 - \tau_{ji})$ , respectively. In the radiation equations, the gas temperature is indexed to the SCDAP/RELAP5 vapor temperature in the hydrodynamic volume in which the SCDAP component exists.

From the view factor reciprocity relation,

$$A_i F_{ij} = A_j F_{ji} . \quad (4-14)$$

Equation (4-13) is simplified to

$$I_{ij} = \left[ E_j^I F_{ij} + E_{ji}^A \frac{A_j}{A_i} \right] \tau_{ji} + \epsilon_{gji} T_g^4 \sigma F_{ij} . \quad (4-15)$$

Substituting the expression for  $I_{ji}$  in Equation (4-10)

$$E_{ij}^A = \mu_i (1 - \epsilon_i) \left[ (E_j^I F_{ij} + E_{ji}^A \frac{A_j}{A_i}) \tau_{ji} + \epsilon_{gji} T_g^4 \sigma F_{ij} \right] . \quad (4-16)$$

By interchanging the i and j in Equation (4-16), an expression for  $E_{ji}^A$  is obtained

$$E_{ji}^A = \mu_j (1 - \epsilon_j) \left[ (E_j^I F_{ji} + E_{ij}^A \frac{A_i}{A_j}) \tau_{ij} + \epsilon_{gij} T_g^4 \sigma F_{ji} \right] . \quad (4-17)$$

Eliminating  $E_{ji}^A$  from Equations (4-16) and (4-17), the expression for  $E_{ij}^A$  is obtained

$$E_{ij}^A = \frac{\mu_i (1 - \epsilon_i) F_{ij} \{ [E_j^I + \mu_j (1 - \epsilon_j) E_i^I \tau_{ij}] \tau_{ij} + \sigma \epsilon_{gij} T_g^4 [1 + \mu_j (1 - \epsilon_j) \tau_{ji}] \}}{[1 - \mu_i (1 - \epsilon_i) \mu_j (1 - \epsilon_j) \tau_{ij} \tau_{ji}]} . \quad (4-18)$$

Combining Equations (4-12) and (4-13), a relation for  $E_i^I$  is obtained

$$E_i^I = \frac{\epsilon_i \sigma T_i + (1 - \mu_i) (1 - \epsilon_i) \sum_{j=1}^n F \{ [E_j + \mu_j (1 - \epsilon_j) \tau_{ij} E_i] \tau_{ji} + \sigma \epsilon_{gji} T_g^4 [1 + \mu_j (1 - \epsilon_j) \tau_{ij}] \}}{[1 - \mu_i (1 - \epsilon_i) \mu_j (1 - \epsilon_j) \tau_{ij} \tau_{ji}]} . \quad (4-19)$$

Equation (4-17) is written in the following form:

$$\begin{aligned} \sum_{j=1}^n \left\{ \left[ 1 - \sum_{k=1}^n \frac{(1 - \mu_i) (1 - \epsilon_i) \mu_k (1 - \epsilon_k) \tau_{ki} \tau_{ik} F_{ik}}{1 - \mu_i (1 - \epsilon_i) \mu_k (1 - \epsilon_k) \tau_{ki} \tau_{ik}} \right] \delta_{ij} - \frac{(1 - \mu_i) (1 - \epsilon_i) \tau_{ji} F_{ij}}{1 - \mu_i (1 - \epsilon_i) \mu_j (1 - \epsilon_j) \tau_{ji} \tau_{ij}} \right\} E_j^I \\ = \epsilon_i \sigma T_i^4 + \sigma (1 - \mu_i) (1 - \epsilon_i) \sum_{j=1}^n \frac{\epsilon_{gji} T_g^4 [1 + \mu_j (1 - \epsilon_j) \tau_{ij}] F_{ij}}{1 - \mu_i (1 - \epsilon_i) (1 - \epsilon_j) \tau_{ji} \tau_{ij}} \end{aligned} \quad (4-20)$$

where  $\delta_{ij}$  is the Kronecker delta function and is defined as

$$\delta_{ij} = \begin{cases} 1 & \text{when } (i = j) \\ 0 & \text{when } (i \neq j) \end{cases} . \quad (4-21)$$

Equation (4-20) is solved for  $E_j^I$  by using a matrix inversion method.

As mentioned earlier, in the absence of liquid droplets,  $\epsilon_{lji}$  is zero and  $\epsilon_{gji}$  is equal to  $(1 - \tau_{ji})$ . If the radiation exchange is assumed to be isotropic (i.e.,  $\mu_i = 0$  and  $\mu_j = 0$ ) Equation (4-20) becomes

$$\sum_{j=1}^n [\delta_{ij} - (1 - \epsilon_i) \tau_{ji} F_{ij}] E_j = \epsilon_i \sigma T_i^4 + \sigma (1 - \epsilon_i) \sum_{j=1}^n \epsilon_{gji} T_g^4 F_{ij} . \quad (4-22)$$

The surface heat flux  $q_i$  is the difference between the outgoing and incident radiation and can be written as

$$q_i = E_i - I_i . \quad (4-23)$$

Substituting for  $E_i$  from Equation (4-7)

$$q_i = [e \sigma T_i^4 + (1 - \epsilon_i) I_i] - I_i . \quad (4-24)$$

Substituting for  $I_i$  from Equation (4-8)

$$q_i = \epsilon_i \left[ \sigma T_i^4 - \frac{(E_i^I - \epsilon_i \sigma T_i^4)}{(1 - \mu)(1 - \epsilon_i)} \right] = \frac{\epsilon_i}{(1 - \mu)(1 - \epsilon_i)} \{ \sigma T_i^4 [1 - \mu(1 - \epsilon_i)] - E_i^I \} . \quad (4-25)$$

The net heat flux,  $q_i$ , to or from any surface  $i$  consists of two parts, as shown in Figure 4-7. One part is the net heat flux exchange with other surfaces,  $q_{is}$ ; and the other part is the net flux exchange with the coolant gas,  $q_{ig}$ . It implies that whatever net surface to surface heat flux,  $q_{is}$ , is released by the hotter rods gets absorbed by the cooler rods. Therefore,

$$Q_r = \sum_{i=1}^n A_i q_{is} = 0 . \quad (4-26)$$

This leads to the relation

$$Q_t = \sum_{i=1}^n A_i q_i = \sum_{i=1}^n A_i (q_{ig} + q_{is}) = \sum_{i=1}^n A_i q_{ig} + \sum_{i=1}^n A_i q_{is} . \quad (4-27)$$

Substituting for  $\sum_{i=1}^n A_i q_{is}$  from Equation (4-26)

$$Q_t = \sum_{i=1}^n A_i q_{ig} = Q_g . \quad (4-28)$$

This means that the algebraic sum of net heat flux exchange with the surroundings for all the surfaces,  $Q_t$ , equals the total heat absorbed by the coolant gas,  $Q_g$ .

The total energy absorbed by the coolant,  $Q_t$ , can be found by the following relation:

$$Q_t = \sum_{i=1}^n A_i q_i = \sum_{i=1}^n \frac{A_i \epsilon_i}{(1 - \mu_i)(1 - \epsilon_i)} \sigma T_i^4 [1 - \mu_i(1 - \epsilon_i)] - E_i^l. \quad (4-29)$$

The energy absorbed by the gas,  $Q_g$ , is also given by the following relation:

$$Q_g = \sum_{i=1}^n A_i \sum_{j=1}^n [a_{gij} (E_i^l F_{ij} + E_{ij}^A) - \epsilon_{gij} \sigma T_g^4 F_{ij}] \quad (4-30)$$

The first term on the right hand side of Equation (4-30) is the amount of radiation absorbed by the vapor along the path  $i$  to  $j$ . The second term is the amount of radiation emitted by the vapor phase.

#### 4.2.2 View Factors

The following expressions for the view factors have been derived using the crossed string method. This method is described in several textbooks.<sup>20,21</sup> Cox,<sup>22</sup> Mandell,<sup>23</sup> and Evans<sup>24</sup> have used this method to derive view factors between rods for nuclear reactor applications. With reference to Figure 4-8, the view factor of Rod 1 with respect to Rod 2 (closest to Rod 1),  $F_{12}$ , is given by the following:

$$F_{12} = 0.5 + \frac{R_2 - R_1}{2\pi R_1} \cos^{-1} \left[ \frac{R_2 - R_1}{P_{12}} \right] - \frac{R_1 + R_2}{2\pi R_1} \sin^{-1} \left\{ \frac{[P_{12}^2 - (R_1 + R_2)^2]^{1/2}}{P_2} \right\} + \frac{1}{2\pi R_1} \{ [P_{12}^2 - (R_1 + R_2)^2]^{1/2} - [P_{12}^2 - (R_1 - R_2)^2]^{1/2} \} \quad (4-31)$$

where

$R_1, R_2, \dots$  = the radii of Rods 1, 2, ... respectively (m)

$P_{12}, P_{23}, \dots$  = the pitches between Rods 1 and 2, Rods 2 and 3, ... respectively (m).

For  $R_1 = R_2 = R$  and  $P_{12} = P$ , Equation (4-31) reduces to the following:

$$F_{12} = 0.5 - \frac{1}{\pi} \sin^{-1} \left[ \frac{(P^2 - 4R^2)^{1/2}}{P} \right] + \frac{1}{2\pi R} [(P^2 - 4R^2)^{1/2} - P] \quad (4-32)$$

For diagonally located rods, the view factor  $F_{13}$  (refer to Figure 4-8) is given by the following

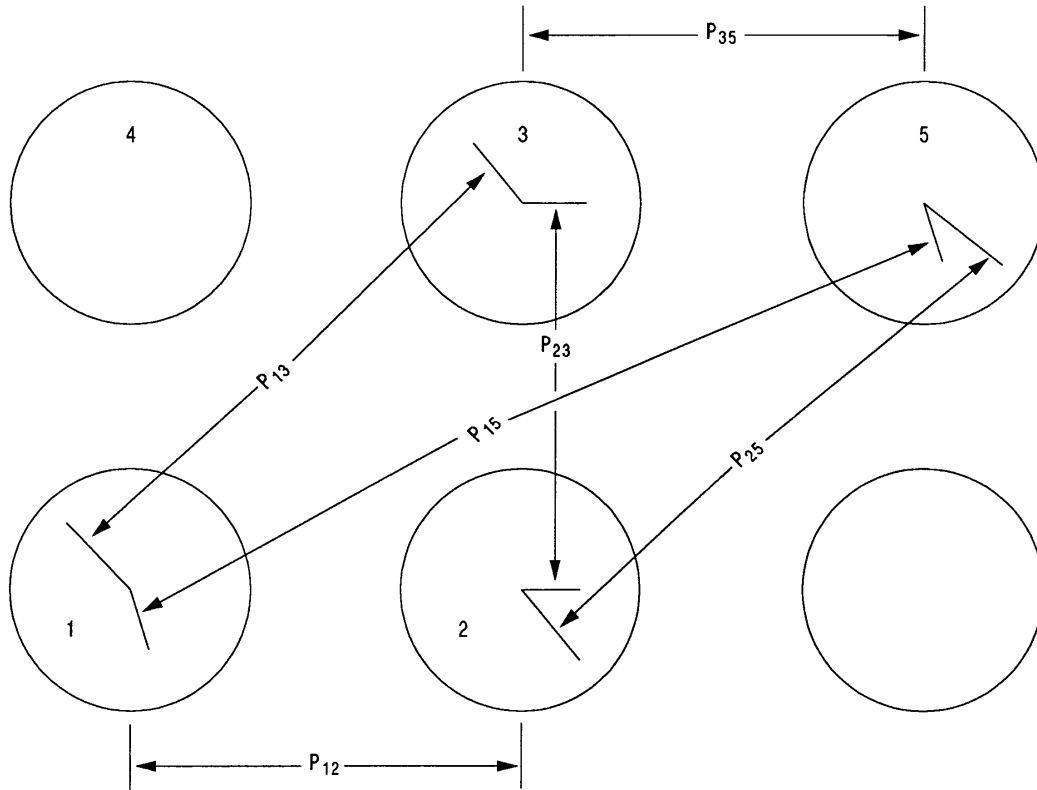


**Figure 4-8.** Geometry for determining view factors between rods.

relation, which can be derived using the crossed string method:

$$\begin{aligned}
 F_{13} = & \left\{ 2\sqrt{P_{13}^2 - (R_1 + R_3)^2} - \sqrt{P_{12}^2 - (R_1 + R_2)^2} - \sqrt{P_{23}^2 - (R_2 + R_3)^2} \right. \\
 & - \sqrt{P_{34}^2 - (R_3 + R_4)^2} - \sqrt{P_{14}^2 - (R_1 + R_4)^2} \\
 & + R_2 \left[ -\frac{\pi}{2} + \sin^{-1} \left( \frac{\sqrt{P_{12}^2 - (R_1 + R_2)^2}}{P_{12}} \right) + \sin^{-1} \left( \frac{\sqrt{P_{23}^2 - (R_2 + R_3)^2}}{P_{23}} \right) \right] \\
 & + R_4 \left[ -\frac{\pi}{2} + \sin^{-1} \left( \frac{\sqrt{P_{34}^2 - (R_3 + R_4)^2}}{P_{34}} \right) + \sin^{-1} \left( \frac{\sqrt{P_{14}^2 - (R_1 + R_4)^2}}{P_{14}} \right) \right] \\
 & + R_1 \left[ \frac{\pi}{2} + \sin^{-1} \left( \frac{\sqrt{P_{12}^2 - (R_1 + R_2)^2}}{P_{12}} \right) + \sin^{-1} \left( \frac{\sqrt{P_{14}^2 - (R_1 + R_4)^2}}{P_{14}} \right) \right] \\
 & + R_3 \left[ \frac{\pi}{2} + \sin^{-1} \left( \frac{\sqrt{P_{23}^2 - (R_2 + R_3)^2}}{P_{23}} \right) + \sin^{-1} \left( \frac{\sqrt{P_{34}^2 - (R_3 + R_4)^2}}{P_{34}} \right) \right] \Bigg\}
 \end{aligned}$$

$$-2 (R_1 + R_3) \sin^{-1} \left( \frac{\sqrt{P_{13}^2 - (R_1 + R_3)^2}}{P_{13}} \right) \left\} \frac{1}{4\pi R_1} . \quad (4-33)$$

For  $R_1 = R_2 = R_3 = R_4 = R$ ,  $P_{12} = P_{23} = P_{34} = P_{41} = P$ , and  $P_{13} = P_{24} = \sqrt{2P}$ , Equation (4-33) simplifies to the following form:

$$F_{13} = \frac{1}{2\pi R} \left\{ \begin{aligned} & \sqrt{2P^2 - R^2} - 2\sqrt{P^2 - R^2} + R \left[ -\frac{\pi}{2} + 2 \sin^{-1} \left( \frac{\sqrt{P^2 - R^2}}{P} \right) \right] + \\ & + R \left[ \frac{\pi}{2} + 2 \sin^{-1} \left( \frac{\sqrt{P^2 - R^2}}{P} \right) \right] - 2R \sin^{-1} \left( \frac{\sqrt{2P - R^2}}{\sqrt{2P}} \right) \end{aligned} \right\} \quad (4-34)$$

Derivation of view factors of a third nearest rod (Figure 4-8),  $F_{15}$ , is similar to that for the diagonal rod:

$$F_{15} = \left\{ \begin{aligned} & 2\sqrt{P_{15}^2 - (R_1 + R_5)^2} - \sqrt{P_{12}^2 - (R_1 + R_2)^2} - \sqrt{P_{25}^2 - (R_2 + R_5)^2} \\ & - \sqrt{P_{35}^2 - (R_3 + R_5)^2} - \sqrt{P_{13}^2 - (R_1 + R_3)^2} \\ & + R_1 \left[ \frac{\pi}{4} + \sin^{-1} \left( \frac{\sqrt{P_{12}^2 - (R_1 + R_2)^2}}{P_{12}} \right) + \sin^{-1} \left( \frac{\sqrt{P_{13}^2 - (R_1 + R_3)^2}}{P_{13}} \right) - 2\sin^{-1} \left( \frac{\sqrt{P_{15}^2 - (R_1 + R_5)^2}}{P_{15}} \right) \right] \\ & + R_3 \left[ -\frac{\pi}{4} + \sin^{-1} \left( \frac{\sqrt{P_{25}^2 - (R_2 + R_5)^2}}{P_{25}} \right) + \sin^{-1} \left( \frac{\sqrt{P_{35}^2 - (R_3 + R_5)^2}}{P_{35}} \right) - 2\sin^{-1} \left( \frac{\sqrt{P_{15}^2 - (R_1 + R_5)^2}}{P_{15}} \right) \right] \\ & - R_2 \left[ \frac{\pi}{4} - \sin^{-1} \left( \frac{\sqrt{P_{12}^2 - (R_1 + R_2)^2}}{P_{12}} \right) + \sin^{-1} \left( \frac{R_2 + R_5}{P_{25}} \right) \right] \\ & - R_3 \left[ \frac{\pi}{4} - \sin^{-1} \left( \frac{\sqrt{P_{35}^2 - (R_3 + R_5)^2}}{P_{35}} \right) + \sin^{-1} \left( \frac{R_1 + R_3}{P_{13}} \right) \right] \end{aligned} \right\} \left( \frac{1}{4\pi R_1} \right) . \quad (4-35)$$

For  $R_1 = R_2 = R_3 = R_5 = R$ , the relation for view factor  $F_{15}$  simplifies to the following:

$$F_{15} = \frac{1}{4\pi R} [2\sqrt{P_{15}^2 - 4R^2} - \sqrt{P_{12}^2 - 4R^2} - \sqrt{P_{25}^2 - 4R^2} - \sqrt{P_{35}^2 - 4R^2} - \sqrt{P_{13}^2 - 4R^2}]$$

$$\begin{aligned}
& + \frac{1}{4\pi} \left[ 2\sin^{-1} \left( \frac{\sqrt{P_{12}^2 - 4R^2}}{P_{12}} \right) + 2\sin^{-1} \left( \frac{\sqrt{P_{35}^2 - 4R^2}}{P_{35}} \right) + \sin^{-1} \left( \frac{\sqrt{P_{15}^2 - 4R^2}}{P_{15}} \right) + \sin^{-1} \left( \frac{\sqrt{P_{25}^2 - 4R^2}}{P} \right) \right] \\
& - \frac{1}{\pi R} \left[ \sin^{-1} \left( \frac{\sqrt{P_{15}^2 - 4R^2}}{P_{15}} \right) - \sin^{-1} \left( \frac{2R}{P_{25}} \right) - \sin^{-1} \left( \frac{2R}{P_{13}} \right) \right]
\end{aligned} \quad (4-36)$$

For the rods placed in a square geometry, this expression is further simplified to the following. In this case,

$$P_{12} = P_{35} = P, P_{25} = P_{13} = \sqrt{2P} \text{ and } P_{15} = \sqrt{5P}.$$

$$\begin{aligned}
F_{15} = & \frac{1}{4\pi R} \left[ 2\sqrt{5P^2 - 4R^2} - 2\sqrt{2P - 4R^2} - 2\sqrt{P^2 - 4R^2} + 4\sin^{-1} \frac{\sqrt{P^2 - 4R^2}}{P} - 2\sin^{-1} \frac{\sqrt{5P - 4R^2}}{\sqrt{5P}} + \sin^{-1} \frac{\sqrt{2P - 4R^2}}{\sqrt{2P}} \right] \\
& + \frac{1}{2\pi} \left[ \sin^{-1} \left( \frac{\sqrt{P^2 - 4R^2}}{P} \right) - 2\sin^{-1} \left( \frac{\sqrt{5P^2 - 4R^2}}{5P} \right) - 2\sin^{-1} \left( \frac{\sqrt{2R}}{P} \right) \right].
\end{aligned} \quad (4-37)$$

All the view factors described above are for cylindrical rods of infinite length. According to Juul,<sup>25</sup> for a typical reactor core  $\frac{P}{R} \approx 3.0$  the application of infinite length view factors to a case of finite length does not cause any significant error (~5%). Therefore, it is reasonable to use Equations (4-31) through (4-37) to calculate view factors for rods of finite length.

To evaluate view factors between all the rods in a bundle, the following methodology and assumptions are used.

For any surface in an enclosure, the summation rule,

$$\sum_{j=1}^n F_{ij} = 1 \quad (4-38)$$

must be satisfied. This rule implies that for an enclosure, all the radiant energy leaving any surface must reach other surfaces (including itself). In the present model, no rod sees another rod beyond two rows or columns. This assumption implies that a portion of energy leaving a rod that would have reached some rods lying beyond two rows or columns has to be accounted for elsewhere. Therefore, the residual view factor of a component group is distributed to other component groups in proportion to the original view factors. To calculate the view factor,  $F_{ij}$ , from one component group  $i$  to another component group  $j$ , the following relation is used:

$$F_{IJ} = \frac{1}{N_I} \sum_{i=1}^{N_I} \sum_{j=1}^{N_J} F_{ij} \quad (4-39)$$

where

$$N_I = \text{the number of rods in component group I}$$

$N_J$  = the number of rods in component group J.

All the rods in one component group have the same radius. The view factor evaluation also must satisfy the reciprocity rule,  $A_I F_{IJ} = A_J F_{JI}$ . This rule implies that the ratio of the view factors of two surfaces with each other is equal to the inverse of the ratio of their respective areas. Therefore, the view factors  $F_{IJ}$  for  $I > J$  have been obtained by the reciprocity rule. For  $I < J$ , the view factors are obtained from first principles and by using Equation (4-39). For  $I = J$ , the summation rule is used to obtain the view factor of a component group to itself.

If a shroud is present around a bundle of  $M \times N$  size, only the outermost rows and columns of rods ( $i = 1$  or  $M$ , or  $j = 1$  or  $N$ ) are considered to exchange radiant energy with the shroud. In such a case, the residual view factor for these peripheral rods is accounted for in the view factor to the shroud. Thus, for these rods,  $R_{ii} = 0$ ; but the component group I to which the rod  $i$  belongs can still see itself, that is,  $F_{II}$  can be nonzero. If a rod is missing in the peripheral location of the bundle, the rod next to it in the inner row and column ( $1 < i < M$  or  $1 < j < M$ ) is allowed to exchange energy with the shroud just as a peripheral rod. The view factors of the shroud also have to satisfy the summation and reciprocity rules.

#### 4.2.3 Mean Path Length

According to Siegel and Howell,<sup>20</sup> mean path length is defined as a fictitious length (i.e., the radius of a gas hemisphere) such that the radiation heat flux to the center of its base is equal to the average radiation flux exchange by the gas and two surface areas containing the actual volume of gas.

For any two areas  $A_i$  and  $A_j$  located at a distance of  $S$  (shortest distance along the path of radiation), let  $\beta_i$  and  $\beta_j$  be the angles between the shortest distance line and the normals on the two surfaces, respectively. Then the mean path length,  $L_{ij}$ , can be evaluated by

$$L_{ij} = \frac{1}{a_{gij}} \ln \frac{1}{A_i F_{ij}} \int_{A_i} \int_{A_j} e^{(-a_{gij} S)} \frac{\cos \beta_i \cos \beta_j}{\pi S^2} dA_i dA_j . \quad (4-40)$$

This equation is difficult to evaluate for a reactor vessel with complicated rod geometry. Therefore, as is done for other radiation models,<sup>12,15</sup> the mean path length is taken to be equal to, or a function of, the distance between the two geometries for which the radiation solution is being sought. The path length between any two rods is obtained by the following equation:

$$L_{ij} = P_{ij} - \frac{\pi}{2} (R_i + R_j) . \quad (4-41)$$

To calculate the average path length between two component groups, the path length between any two rods (subcomponents) is weighted by the corresponding view factor. If  $N_I$  and  $N_J$  are the number of rods (subcomponents) in component groups I and J, respectively, then the average path length between any

two component groups I and J is given by (optically this approximation)

$$L_{ij} = \frac{\sum_{i=1}^{N_I} \sum_{j=1}^{N_J} F_{ij} L_{ij}}{\sum_{i=1}^{N_I} \sum_{j=1}^{N_J} F_{ij}} . \quad (4-42)$$

#### 4.2.4 Absorptivities and Emissivities

The absorptivities and emissivities of the surfaces are obtained from MATPRO.

When the cladding surface temperature has not exceeded 1,500 K, the surface emissivity (which equals absorptivity) is modeled by Equations (4-43). For oxide layer thicknesses of  $3.88 \times 10^{-6}$  m or greater,

$$\epsilon_1 = 0.808642 - 50.0 d. \quad (4-43)$$

where

$\epsilon_1$  = hemispherical emissivity (unitless)

$d$  = oxide layer thickness (m).

When the maximum cladding temperature has exceeded 1,500 K, emissivity is taken to be the larger of 0.325 and

$$\epsilon_2 = \epsilon_1 \exp \left[ \frac{1500 - T}{300} \right] \quad (4-44)$$

where

$\epsilon_1$  = value for emissivity obtained from Equation (4-43)

$T$  = maximum cladding temperature (K).

Zirconium oxide thickness would be expected to vary from zero to about 900  $\mu\text{m}$ . A value of 300  $\mu\text{m}$  is taken that results in an average value of  $\epsilon_1$  of 0.7936. At present, the shroud surface is assumed to have the same radiation properties as the fuel rods.

Vapor absorptivities and emissivities are calculated in the same manner as is done in the TRAC-BD1 code. For vapor, the absorption coefficient  $K_{gij}$  is evaluated after determining emissivity and absorptivity

$$K_{gij} = \frac{\ln(1 - a_{gij})}{L_{ij}} . \quad (4-45)$$

At present, the emissivity and absorptivity of the gaseous medium are obtained in a manner similar to that used in TRAC-BD1. That method is reproduced here for the sake of completeness.

The emissivity of an absorbing gaseous medium for monochromatic radiation of wave length  $\lambda$  is given by the following equation:

$$\epsilon_{\lambda} = 1 - e^{(-K_{\lambda} p L_{ij})} \quad (4-46)$$

where

$p$  = pressure (Pa)

$K_{\lambda}$  = spectral absorption coefficient  $(\text{Pa} \times \mu\text{m})^{-1}$ .

The total hemispherical emittance is defined as the ratio of the emissive power  $e$  of a given surface to that of a black surface  $e_b$  at the same temperature.

$$e_g = \frac{e}{e_b} = \frac{\int_0^{\infty} \epsilon_{\lambda} e_{b\lambda}(T) d\lambda}{\int_0^{\infty} e_{b\lambda}(T) d\lambda} = \frac{\int_0^{\infty} \epsilon_{\lambda} e_{b\lambda}(T) d\lambda}{\sigma T^4} \quad (4-47)$$

The Planck function,  $e_{b\lambda}$ , is given by

$$e_{b\lambda} = \frac{\frac{2\pi h C^2}{\lambda^3}}{e^{\left(\frac{hC}{\lambda kT}\right)} - 1} \quad (4-48)$$

where

$h$  = Planck's constant,  $(6.625 \times 10^{-34} \text{ J}\cdot\text{s})$

$k$  = Boltzmann's constant  $(1.38 \times 10^{-23} \text{ J/K})$

$C$  = the speed of light in the medium, speed of light in vacuum/refractive index of the medium  $(2.998 \times 10^8 \text{ m/s})/\text{refractive index of the medium}$ .

The absorptivity,  $a_{\lambda}$ , of the medium is obtained by evaluating an equation similar to that for emissivity at the temperature of the surface emitting the radiation incident on the absorbing medium.

$$a_{\lambda} = \frac{\int_0^{\infty} a e_{b\lambda}(T_s) d\lambda}{\sigma T_s^4} \quad (4-49)$$

where  $a_\lambda = \epsilon_\lambda$  by Kirchhoff's law in thermodynamic equilibrium.

The absorption spectrum of water vapor is considered to consist of six major absorption bands, as reported by Hottel and Sarofim.<sup>26</sup> Table 4-1 shows the wave length and absorption coefficients,  $K_{\lambda_o}$ , of these bands at 300 K. At other temperatures, absorption coefficients can be obtained by

$$K_\lambda = K_{\lambda_o} \left( \frac{300}{T} \right) . \quad (4-50)$$

The values of  $K_\lambda$  used in the present model are assumed to be constant within each wave length band and zero elsewhere. Therefore, integral relations for emissivity and absorptivity can be approximated as the sums over the wavelength bands given in Table 4-1.

**Table 4-1.** Water vapor absorption.

Wavelength at band center ( $\mu\text{m}$ )	Minimum wavelength ( $\mu\text{m}$ )	Maximum wavelength ( $\mu\text{m}$ )	Absorption coefficient $K_{\lambda_o}$ ( $\text{Pa} \times \mu$ ) <sup>-1</sup>
1.1	1.1017	1.1809	0.523
1.38	1.3243	1.4405	13.42
1.87	1.7693	1.9829	16.38
2.87	2.495	2.942	204.19
6.3	5.2854	7.7942	283.64
20.0	12.43	51.1509	94.65

$$\epsilon_g = \frac{1}{\sigma T^4} \sum_{i=1}^6 \epsilon_{\lambda_i} e_{\lambda_i} (T) \Delta\lambda_i \quad (4-51)$$

$$a_g = \frac{1}{\sigma T_s^4} \sum_{i=1}^6 \epsilon_{\lambda_i} e_{\lambda_i} (T_s) \Delta\lambda_i \quad (4-52)$$

where

- $i$  = wavelength band index
- $e_{\lambda_i}$  = average value of the Planck black body function evaluated at the wavelength at band center
- $T$  = temperature of the gaseous medium
- $T_s$  = surface temperature.

### 4.3 Nuclear Heat Model

For each SCDAP component, the user may select either the SCDAP model or one of the RELAP5 power options to calculate nuclear heat. The following discussion refers to the SCDAP nuclear heat model.

The energy release from fissioning of uranium is manifested in a variety of forms. Table 4-2 lists recoverable forms of energy from thermal fissioning of  $^{235}\text{U}$  that are considered in the nuclear heat model and average energy per fission associated with each form. The Evaluated Nuclear Data File<sup>27</sup> is the source of information for the first four forms of energy in Table 4-2, and the ANSI/ANS-5.1-1979 decay heat standard<sup>28</sup> is the source for the fifth form of energy listed. The first three forms of energy in Table 4-2 are released at the time the fission event and are collectively known as prompt nuclear heat. They account for about 92% of the recoverable fission energy. The remaining two forms of energy in Table 4-2 appear at some time after the fission event and are classified as delayed nuclear heat. This energy is due to the radioactive decay of a large number of different fission products and actinides ( $^{239}\text{U}$  and  $^{239}\text{Np}$  in this model). Since radioactive decay is a random event that is characterized by an exponential probability distribution, the delayed nuclear heat is exponentially distributed in time following a fission event.

**Table 4-2.** Energy release from fission of  $^{235}\text{U}$ .<sup>a</sup>

Form		Energy (MeV/fission)
I	Kinetic energy of fission products (prompt)	169.58
II	Fission $\gamma$ -rays (prompt)	6.96
III	Kinetic energy of fission neutrons (prompt)	4.79
IV	Fission product decay (delayed)	
	$\beta$	6.43
	$\gamma$	6.26
	Neutrons (kinetic energy)	0.0071
V	Neutron capture activation (delayed)	
	Fission Products	~.5
	Actinides	~.8

a. Total from forms I, II, and III = 181.33 MeV/fission (prompt). Total from forms IV and V = 14 MeV/fission (delayed, recoverable). Energy from neutrons is non-recoverable.

Prompt nuclear heat is determined by thermal neutron flux levels. Because neutron flux distributions are not determined by the code, the nuclear heat model requires that any prompt nuclear heat generated during the problem time be input to the model. Delayed nuclear heat is determined by the prior operating history. This is provided as input to the model by specifying the rod average total (prompt plus delayed) volumetric power for each time span prior to the start of the problem. For nonfuel rod components (i.e., control rods or structural material), the user must supply total power for the problem time period. For fuel rods, the user has the option of supplying total power for the problem time period and thus overriding

the decay heat calculations. Additional required input information are fuel enrichment, fuel density, rate of  $^{239}\text{U}$  production (ratio of fission producing neutron absorption in  $^{238}\text{U}$ ), and axial and radial multiplication factors that convert the rod average prompt and delayed power to local power.

This model determines the delayed nuclear heat based on the ANSI/ANS-5.1-1979 decay heat standard, and the required nuclear data are based on the Evaluated Nuclear Data File. Neither the delayed nuclear heat from neutron capture in structural material nor the energy added by fissioning due to delayed neutrons subsequent to reactor shutdown are considered. However, the user can force consideration of these effects by specifying their contributions as an additional prompt nuclear heat source. The delayed nuclear heat model is based on the following major assumptions:

- The fuel rods are of commercial LWR design.
- The bundle component remains intact and at initial density and volume. Movement of material due to fuel rod disruption is accounted for outside of this model by the SCDAP subroutines FSTATE and CFDAMG, depending on the state of the bundle. These routines maintain an inventory system that will trace a piece of material back to its original location in order to determine the current decay power. (The prompt power is not history dependent; therefore, only the current location peaking factor and average power are required to determine current prompt power.)
- $^{235}\text{U}$  is the only fissile material.
- $^{238}\text{U}$  is the only fertile material. (This implies that the only actinide decay chain that will be considered is the  $^{239}\text{U}$  to  $^{239}\text{Pu}$  decay chain due to  $^{238}\text{U}$  neutron absorption.)
- Gamma energy is completely recoverable with a flat radial distribution and the user supplied axial distribution of energy deposition.

Most of the computations required for this model, including those for establishing the ANS-5.1-based delayed nuclear heat, are performed during initialization. These computations establish power history tables and axial and radial distribution tables. The volumetric power for any time and location within the analysis is determined by interpolating these tables.

The total nuclear heat source due to fissioning is represented as

$$Q(z,r,t) = Q_p(t) Z_p(z) R_p(r) + Q_d(t) Z_d(z) R_d(r) \quad (4-53)$$

where

$Q(z,r,t)$  = total nuclear heat at axial position  $z$  and radial position  $r$  of the component at time  $t$  ( $\text{W}/\text{m}^3$ )

$Q_p(t)$  = component average prompt nuclear heat at time  $t$  ( $\text{W}/\text{m}^3$ )

$Z_p(z)$  = axial peaking factor for prompt heat at position  $z$

$R_p(r)$  = radial peaking factor for prompt heat at position  $r$

$Q_d(t)$  = component average delayed nuclear heat at time  $t$  ( $\text{W}/\text{m}^3$ )

$$\begin{aligned} Z_d(z) &= \text{axial peaking factor for delayed heat at position } z \\ R_d(r) &= \text{radial peaking factor for delayed heat at position } r. \end{aligned}$$

For a fuel rod component, the user must supply the three factors of the first term of Equation (4-53) ( $Q_p$ ,  $Z_p$ ,  $R_p$ ) as well as the factor  $Z_d$  from the second term of the equation. The user may either supply  $Q_d$  or allow the model to calculate the term. For components other than fuel rods, the user must supply  $Q_d$ .<sup>a</sup> The factor  $R_d$  is always determined by the model, although for components other than fuel rods,  $R_d$  is set equal to  $R_p$ .

The factor  $Z_p$  accounts for the axial distribution of prompt nuclear heat due to the neutron flux distribution. Since  $Z_p$  may shift during the transient, the user can supply separate axial peaking factor arrays for different time periods. Under equilibrium conditions, the distribution of the delayed nuclear heat is the same as the prompt distribution. However, when the prompt distribution changes, the delayed distribution exponentially approaches the new shape with time. Therefore, the delayed distribution may be different from the prompt distribution; the user can input a separate axial nuclear heat distribution for delayed nuclear heat. Since the conditions that cause the radial distribution of prompt heat are not expected to change significantly with time, the user is only allowed to input one prompt radial distribution shape. The model always provides the radial distribution of delayed heat based on the user-supplied prompt radial distribution and the component type (fuel rod or nonfuel rod).

Expanding the second term of Equation (4-53) (delayed nuclear heat) into its components yields

$$Q_d(t) Z_d(z) R_d(r) = (DF - G - Q_{fd} + Q_{Ad}) Z_d(z) R_d(r) \quad (4-54)$$

where

$$\begin{aligned} Q_{fd} &= \text{rod average fission product decay power (W/m}^3\text{)} \\ Q_{Ad} &= \text{rod average actinide (}^{239}\text{U, }^{239}\text{Np) decay power (W/m}^3\text{)} \\ DF &= \text{reduction factor in decay heat due to loss of volatile fission products}^{29} \\ G &= \text{neutron capture correction to fission product decay.} \end{aligned}$$

A comparison of the magnitude of these components is given in Figure 4-9. The reduction in decay power due to loss of volatile fission products is discussed in Reference 29. The remaining components are discussed in the following sections of this report.

#### 4.3.1 Fission Product Decay Power

Reference 28 provides an empirical correlation for the decay power per fission  $t$  seconds after a fission pulse from the thermal fission of  $^{235}\text{U}$ . The form of the correlation is given by

---

a. The user may also supply nonnuclear heat (i.e., electrical) through the terms in Equation (4-53). The delayed nuclear heat model options are not recommended for use in such situations.

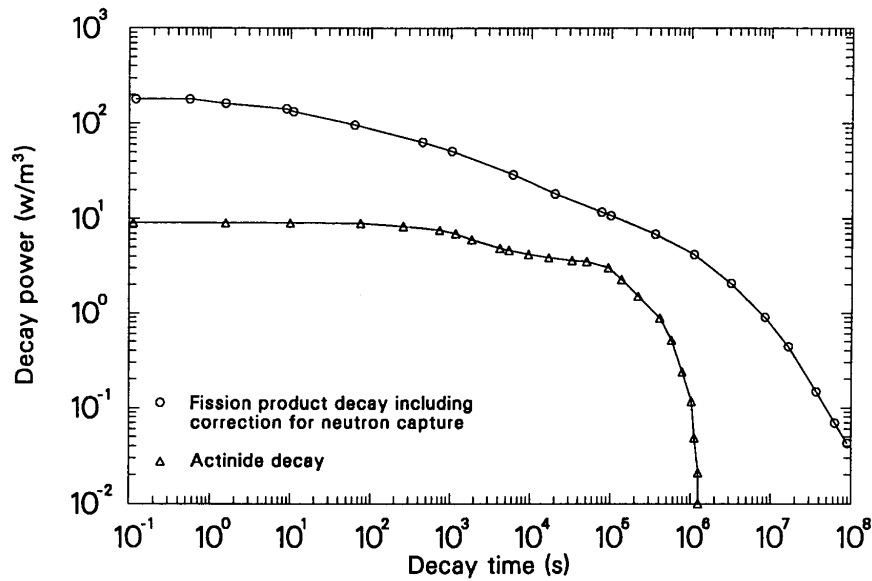


**Figure 4-9.** Comparison of decay heat components.

$$f(t) = \sum_{i=1}^{23} \alpha_i e^{(-\lambda_i t)} \quad (4-55)$$

where

$F(t)$  = decay power per fission  $t$  seconds after a  $^{235}\text{U}$  thermal fission pulse (MeV/fission • s)

$\alpha_i$  = initial decay value of empirical (nonphysical) Group  $i$  (MeV/fission • s)

$\lambda_i$  = time constant of empirical Group  $i$  ( $\text{s}^{-1}$ ).

The constants  $\alpha_i$  and  $\lambda_i$  are given in Table 4-3.

The decay power after an operating period is the product of Equation (4-55) and the fission rate integrated over the operating period  $T$ :

$$Q_{fd}(T) = \int_0^T f(T - T') FR(T') dT' \quad (4-56)$$

where  $FR(T')$  is the fission rate of  $^{235}\text{U}$  at time  $T'$  (fission/ $\text{m}^3 \cdot \text{s}$ ) (W/MeV).

The term  $FR(T')$  is determined by

$$FR(T') = \frac{Q_p(T')}{E_f} = \frac{Q(T') - Q_d(T')}{E_f} \quad (4-57)$$

**Table 4-3.** Decay power correlation constants .

i	$\alpha_i$	$\lambda_i$	i	$\alpha_i$	$\lambda_i$
1	6.5057E-1	2.2138 E+1	13	2.5232 E-6	1.0010 E-5
2	5.1264 E-1	5.1587 E-1	14	4.9948 E-7	2.5438 E-6
3	2.4384 E-1	1.9594 E-1	15	1.8531 E-7	6.6361 E-7
4	1.3850 E-1	1.0312 E-1	16	2.6608 E-8	1.2290 E-8
5	5.5440 E-2	3.3656 E-2	17	2.2398 E-9	2.7213 E-8
6	2.2225 E-2	1.1681 E-2	18	8.1641 E-12	4.3714 E-9
7	3.3088 E-3	3.5870 E-3	19	8.7797 E-11	7.5780 E-10
8	9.3015 E-4	1.3930 E-3	20	2.5131 E-14	2.4786 E-10
9	8.0943 E-4	6.2630 E-4	21	3.2176 E-16	2.2384 E-13
10	1.9567 E-4	1.8906 E-4	22	4.5028 E-17	2.4600 E-14
11	3.2535 E-5	5.4988 E-5	23	7.4791 E-17	1.5699 E-14
12	7.5595 E-6	2.0958 E-5			

where

$Q_p(T')$  = prompt nuclear heat at time  $T'$  (W/m<sup>3</sup>)

$Q(T')$  = total nuclear heat at time  $T'$  (W/m<sup>3</sup>)

$Q_d(T')$  = decay nuclear heat at time  $T'$  (W/m<sup>3</sup>)

$E_f$  = prompt energy per fission of <sup>235</sup>U = 181.33 (MeV/fission).<sup>29</sup>

Substituting Equation (4-55) into Equation (4-56) and breaking the integration into a sum of operating periods for which FR is constant yields

$$Q_{fd}(T) = \sum_{n=1}^N FR_n \left[ \sum_{i=1}^{23} \alpha_i \int_{T_{n-1}}^{T_n} e^{-\lambda_i(T-T')} dT' \right] \quad (4-58)$$

where  $N$  is the number of periods used to represent the time span 0 to  $T$ .

Integrating Equation (4-58) yields

$$Q_{fd}(T) = \sum_{n=1}^N FR_n \left[ \sum_{i=1}^{23} \frac{\alpha_i}{\lambda_i} e^{(-\lambda_i T)} [1 - e^{(-\lambda_i \Delta t_n)}] \right] \quad (4-59)$$

where

$$\Delta t_n = T_n - T_{n-1} \text{ (s).} \quad (4-60)$$

By expanding Equation (4-59), rearranging terms, and separating the decay heat into 23 components, the following may be obtained:

$$Q_{fd,n}^i = Q_{fd,n-1}^i e^{(-\lambda_i \Delta t_n)} + FR_n \frac{\alpha_i}{\lambda_i} [1 - e^{(-\lambda_i \Delta t_n)}] \quad (4-61)$$

where

$$\begin{aligned} Q_{fd,n}^i &= i\text{-th component of decay heat after time step } n \text{ (W/m}^3\text{)} \\ Q_{fd,n-1}^i &= i\text{-th component of decay heat after time step } n-1 \text{ (W/m}^3\text{)}. \end{aligned}$$

The fission product decay heat is now in a form that can be updated each time step given the current fission rate and time step size.

#### 4.3.2 Neutron Capture Correction to Fission Product Decay

Reference 28 provides two empirical methods for determining the neutron capture correction to fission product decay [the factor  $G$  from Equation (4-53)]. One method is a table of values that is valid for shutdown times up to  $10^9$  seconds and operating times up to 4 years for standard LWR operating conditions. The other method is a correlation that is valid for shutdown times up to  $10^4$  seconds, operating times up to 4 years, and fissions per initial fissile atom up to three. The correlation is used for times less than  $10^4$  seconds, since it is more accurate within this range; and the tables are used for times greater than  $10^4$  seconds. The correlation is given by

$$G = 1.0 + (3.24 \times 10^{-6} + 5.23 \times 10^{-10} t) T^{0.4} \Psi \quad (4-62)$$

where

$$\begin{aligned} G &= \text{neutron capture correction to fission product decay} \\ t &= \text{time since shutdown (s)} \\ T &= \text{operating time (s)} \\ \Psi &= \text{fissions per initial fissile atom.} \end{aligned}$$

The term  $\Psi$  is determined from the operating history by

$$\Psi = \frac{1}{v} \int_0^T FR dT' \quad (4-63)$$

where

$$\begin{aligned} v &= \text{number of initial fissile atoms per unit volume (atoms/m}^3\text{)} \\ FR &= \text{fission rate per volume (fissions/m}^3\text{•s).} \end{aligned}$$

The term  $v$  is determined from the fuel pellet initial conditions by

$$v = \frac{w\rho N_o}{At} \quad (4-64)$$

where

$$\begin{aligned} w &= \text{weight fraction of } ^{235}\text{UO}_2 \\ \rho &= \text{fuel pellet density (kg/m}^3\text{)} \\ N_o &= \text{Avogadro's number, } 6.023 \times 10^{26} \text{ (molecule/kg•mole)} \\ At &= \text{atomic weight of } ^{235}\text{UO}_2. \end{aligned}$$

The table of values that are interpolated when conditions are outside the range of Equation (4-62) is shown in Table 4-4.

**Table 4-4.** G factors for times greater than 10,000 s.

Time After Shutdown (s)	G	Time after shutdown (s)	G
1.0	1.020	4.0 E4	1.098
1.5	1.020	6.0 E4	1.111
2.0	1.020	8.0 E4	1.119
4.0	1.021	1.0 E5	1.124
6.0	1.022	1.5 E5	1.130
8.0	1.022	2.0 E5	1.131
10.0	1.022	4.0 E5	1.126
15.0	1.022	6.0 E5	1.124
20.0	1.022	8.0 E5	1.123
40.0	1.022	1.0 E6	1.124
60.0	1.022	1.5 E6	1.125

**Table 4-4.** G factors for times greater than 10,000 s. (Continued)

Time After Shutdown (s)	G	Time after shutdown (s)	G
80.0	1.022	2.0 E6	1.127
1.0 E+2	1.023	4.0 E6	1.134
1.5 E+2	1.024	6.0 E6	1.146
2.0 E+2	1.025	8.0 E6	1.162
4.0 E+2	1.028	1.0 E7	1.181
6.0 E+2	1.030	1.5 E7	1.233
8.0 E+2	1.032	2.0 E7	1.284
1.0 E+3	1.033	4.0 E7	1.444
1.5 E+3	1.037	6.0 E7	1.535
2.0 E+3	1.039	8.0 E7	1.586
4.0 E+3	1.048	1.0 E8	1.598
6.0 E+3	1.054	1.5 E8	1.498
8.0 E+3	1.060	2.0 E8	1.343
1.0 E+4	1.064	4.0 E8	1.065
1.5 E+4	1.074	6.0 E8	1.021
2.0 E+4	1.081	8.0 E8	1.012

### 4.3.3 Actinide Decay Power

The actinide decay term in Equation (4-54) is calculated using the model supplied in Reference 28. This model assumes that the actinide decay power is due only to the decay of  $^{239}\text{U}$  and  $^{239}\text{Np}$ . The actinide power is given by

$$Q_{\text{Ad}} = \frac{Q_f}{E_f} [F_{^{239}\text{U}}(t, T) + F_{^{239}\text{Np}}(t, T)] \quad (4-65)$$

where

$$\begin{aligned} Q_f &= \text{total maximum}^a \text{ fission power during the operating history (W/m}^3\text{)} \\ E_f &= \text{effective energy release per fission (195.3 MeV/fission)} \end{aligned}$$

a. Use of total maximum fission power is specified by Reference 29.

$F = {}^{239}\text{U}$  or  ${}^{239}\text{Np}$  decay energy per fission (MeV/fission).

The terms  $F_{\text{U}239}$  and  $F_{\text{NP}239}$  are given by

$$F_{239_{\text{U}}}(t, T) = RE_{239_{\text{U}}}(1 - e^{-\lambda_1 T})e^{-\lambda_1 t} \quad (4-66)$$

$$F_{239_{\text{NP}}}(t, T) = RE_{239_{\text{NP}}} \frac{\lambda_1}{\lambda_1 - \lambda_2} (1 - e^{-\lambda_2 T})e^{-\lambda_2 t} - \frac{\lambda_2}{\lambda_1 - \lambda_2} (1 - e^{-\lambda_1 T})e^{-\lambda_1 t} \quad (4-67)$$

where

$R = {}^{239}\text{U}$  of production per fission (atoms/fission)

$T =$  operating time (s)

$t =$  time since shutdown (s)

$E_{239_{\text{U}}} =$  average decay energy of  ${}^{239}\text{U}$  (0.474 MeV)

$E_{239_{\text{NP}}} =$  average decay energy of  ${}^{239}\text{Np}$  (0.419 MeV)

$\lambda_1 =$   ${}^{239}\text{U}$  decay constant ( $4.91 \text{ E-}4 \text{ s}^{-1}$ )

$\lambda_2 =$   ${}^{239}\text{Np}$  decay constant ( $3.42 \text{ E-}6 \text{ s}^{-1}$ ).

#### 4.3.4 Radial Peaking Factor for Delayed Heat

For nonfuel components, the radial distribution of delayed power,  $R_d(r)$ , is set equal to radial distribution of prompt power,  $R_p(r)$ . However, for fuel rods,  $R_d(r)$  is not identical to  $R_p(r)$  because  $\gamma$ -ray energy may be deposited a considerable distance from the location of generation. Since  $\gamma$ -ray energy is about one-half of the delayed power,  $R_d(r)$  within a fuel rod is estimated by

$$R_d(r) = 0.5 [1 + R_p(r)] . \quad (4-68)$$

The overall radial power distribution is determined by

$$R^j = \frac{(GQ_{fd} + Q_{Ad})Z_d^j(1 + R_p)\sqrt{1 + R_p} + Q_p Z_p^j R_p}{(GQ_{fd} + Q_{Ad})Z_d^j + Q_p Z_p^j} \quad (4-69)$$

where the superscript  $j$  denotes axial position and is required due to the possible difference in prompt and delayed axial power distributions.

## 4.4 Special Techniques

### 4.4.1 Time Step Control

In the past, SCDAP has not had the capability of repeating the time step used within SCDAP/RELAP5; whatever time step that was selected for RELAP5 was automatically used in SCDAP. This caused stability problems when, as an example, the SCDAP heat structure is radiating energy into RELAP5 hydrodynamic volume. In this case both SCDAP and RELAP5 need to use a smaller time step determined by the heat flux from SCDAP heat structures into RELAP5 volumes. Hence, the correct approach is to treat SCDAP heat structures the same as RELAP5 heat structures in the program structure and allow SCDAP to have the capability to automatically adjust the time step according to its own criteria. This capability has been implemented in SCDAP/RELAP5/MOD3.1.

Figure 4-10 repeats the SCDAP/RELAP5 top level organization as discussed in Section 2. In implementing the time step repetition and time step control logic, the call to the SCDAP subcode has been split into two parts, SCDPRH (SCDAP Pre-HYDRO) and SCDPSH (SCDAP Post-HYDRO). The Pre-HYDRO portion of the code is the section of coding that has the capability of declaring the current time advancement unsuccessful, and repeating the advancement with a smaller time step. Hence, the new calling sequence allows both SCDAP and RELAP5 to run at a smaller time step if the success criterion is not met in HYDRO.

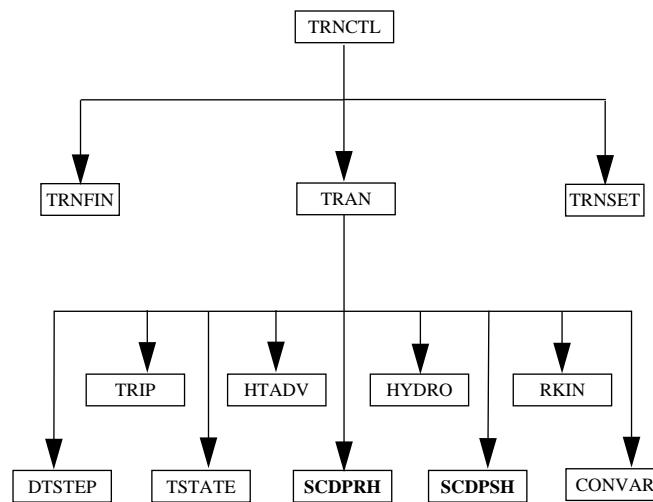


**Figure 4-10.** SCDAP/RELAP5 top level organization.

SCDAP also has the capability of repeating a time step if it is detected in SCDADV that the current time step is greater than the maximum time step allowed by the stability criterion due to the explicit coupling between radiation heat transfer from SCDAP heat structure and RELAP5 hydrodynamics. Various checks on solution acceptability are also used to control the time step. These include material Courant limit checks, mass error checks, material properties out of defined ranges, water property errors, or excessive extrapolation of state properties in the meta-stable regimes.

The material Courant limit check is made before a hydrodynamic advancement takes place. The material Courant limit is evaluated for each hydrodynamic volume using the volume mass average velocity, i.e.,

$$(\Delta t_c)_i = \left[ \Delta x \frac{\max(\alpha_f^n, \alpha_g^n)}{\max(|\alpha_f^n V_f^n|, |\alpha_g^n V_g^n|)} \right], i = 1, 2, \dots, n \quad (4-70)$$

where  $n$  is the total number of volumes in the entire system.

The minimum of the Courant limit for each of the volumes is the Courant limit for the entire system.

The mass error check is made after the time step solution is nearly complete. Two types of mass error measures are computed. The first one checks the validity of density linearization and is defined as

$$E_m = \max \left[ \left( \frac{|\rho_{mi} - \rho_i|}{\rho_i} \right), i \right] = 1, 2, \dots, n \quad (4-71)$$

where  $\rho_{mi}$  is the total density of the  $i^{\text{th}}$  volume computed from the state relationship. The second one is a measure of overall system mass error and is given by

$$E_{rms} = 2 \frac{\sum_{i=1}^N [V_i (\rho_i - \rho_{mi})]^2}{\sum_{i=1}^N (V_i \rho_i)^2} \quad (4-72)$$

where  $V_i$  is the volume of the  $i^{\text{th}}$  volume.

If either  $E_m$  or  $E_{rms}$  is  $> 0.008$ , the time step is rejected and repeated with one half of the time step size. Otherwise, the time step is accepted; and the next time step size is doubled if both  $E_m$  and  $E_{rms}$  are  $< 0.0008$ .

At any point in the solution flow, if a material property is found to lie outside the defined range, then the time step is halved and repeated. This process will proceed until the user-specified minimum time step is reached. If the minimum time step is reached without obtaining a valid solution, then the code calculation is terminated, and the last time step is repeated with a diagnostic dump printed. A program stop is encountered at completion of the step. This same procedure is applied for all property or extrapolation features.

#### 4.4.2 Radiation Stability Limits

Experience has shown that instability can occur in the hydrodynamic solution at time steps less than the Courant limit. As an example, in the transmittal problem input#0 the convective Courant limit, as

determined by  $\max [ |v_g|, |v_f| ] \frac{dt}{dx}$ , is 1.2 seconds. Hence, this problem can, in principle, be run with a time step of 0.5 seconds using the semi-implicit method without fear of incurring stability problems. However, experience has shown that this is only true with radiation heat transfer disabled. This suggests that there is another stability limit in the vapor energy equation in the semi-implicit method. Ignoring the variations in the voids, temperatures, densities, and the interfacial heat transfer terms in the vapor energy equation, the finite-difference form of that equation is

$$U_j^{n+1} = \left( 1 - a - \frac{h_r dt A}{mC_v} \right) U_j^n + a U_{j-1}^n \quad (4-73)$$

where

$$\begin{aligned} U_j^{n+1} &= \text{vapor internal energy at volume } j \text{ at the current time step,} \\ U_j^n &= \text{vapor internal energy at volume } j \text{ at the previous time step} \\ U_{j-1}^n &= \text{vapor internal energy at volume } j-1 \text{ at the previous time step} \\ a &= v_g \frac{dt}{dx} \\ A &= \text{surface area of the fuel rod interfacing the volume, and} \end{aligned}$$

$$h_r = \sigma \epsilon (T_{w2}^2 + T_{g2}^2) (T_w + T_g)$$

where

$$\begin{aligned} \sigma &= \text{Stefan-Boltzmann constant} \\ \epsilon &= \text{emissivity of the vapor} \\ T_w &= \text{temperature of the fuel rod interfacing volume } j \\ T_g &= \text{temperature of the vapor at volume } j. \end{aligned}$$

In order for the difference scheme to be stable, the coefficients in the difference equation should be positive, implying that

$$1 - a - \frac{h_r dt A}{mC_v} > 0. \quad (4-74)$$

If the nearly implicit scheme is used, then it can be shown that the scheme is stable if

$$dt < \frac{2mC_v}{h_r A}. \quad (4-75)$$

On the other hand, if the semi-implicit scheme is used, the scheme is stable if

$$\Delta t < \frac{1}{\frac{h_r A}{m C_v} + \frac{v}{dx}}. \quad (4-76)$$

If the term  $\frac{v}{dx}$  is small compared to the term  $\frac{h_r A}{m C_v}$  in the inequality (4-76), the radiation heat flux determines the limiting stability time step.

#### 4.4.3 Radiation Time Smoothing

During the developmental assessment process, oscillations due to numerical instabilities were observed in several parameters calculated by the code. These oscillations occurred with abrupt changes in flow areas or when the heat transfer correlation to a fluid was discontinuous due to the lack of a physical model. Through an investigation, it was determined that discontinuities in the radiation heat transfer to a fluid were the major cause of these oscillations. Various methods of time smoothing were investigated. The method was chosen that smoothed out the oscillations and best reproduced experimental and calculated results. This section describes the model chosen, the algorithm, and the methods used to test the model.

The formula for linear time smoothing is given below.

$$f_{n+1} = e^{-\frac{\Delta t}{\tau}} f_n + \left(1 - e^{-\frac{\Delta t}{\tau}}\right) f_{n+1} \quad (4-77)$$

where

$$\begin{aligned} f_n &= \text{smoothed term at advancement } n \\ \Delta t &= \text{time step} \\ \tau &= \text{time constant for smoothing.} \end{aligned}$$

If time smoothing is applied to the variable  $q_{radab}(i,k)$ , which is the amount of heat input to the fluid by radiation at axial level  $k$  and enclosure  $i$ , we have

$$q_{radab}_{n+1} = e^{-\frac{\Delta t}{\tau}} q_{radab}_n + \left(1 - e^{-\frac{\Delta t}{\tau}}\right) q_{radab}_{n+1}. \quad (4-78)$$

In order to conserve energy, we want, before time smoothing,

$$\sum_j N_j P_{jk} q_{rdsur}_{jk} = q_{radab}_k \quad (4-79)$$

where

- j = component number
- k = axial level
- qrdsur = radiation heat flux of component j at axial node k (w/m<sup>2</sup>)
- N<sub>j</sub> = number of individual rods in component j
- P<sub>jk</sub> = outer surface of component j at axial node k.

We also want

$$\sum_j N_j P_{jk} \text{qrdsur}_{jk}' = \text{qradab}_k' \quad (4-80)$$

where qrdsur' is the corrected radiation flux. The correction is necessary to make sure that energy is conserved.

The default time constant used is 0.01 because this is the theoretical average value of the time elapsed during transition of flow regimes. It was found that the numerical results are not sensitive to the time constant chosen as long as the time constant is between 0.01 and the maximum requested time step.

## 5. REFERENCES

1. T. Heames et al., *VICTORIA: A Mechanistic Model of Radionuclide Behavior in the Reactor Coolant System Under Sever Accident Conditions*, NUREG/CR-5545, SAND90-0756, Rev. 1, December 1992.
2. C. M. Allison, C. S. Miller, and N. L. Wade (Eds.) *RELAP5/MOD3 Code Manual, Volumes I through IV*, NUREG/CR-5535, EGG-2596, DRAFT, June 1990.
3. C. M. Allison and G. H. Beers, "Comparisons of the SCDAP Computer Code with Bundle Data Under Severe Accident Conditions," Seventh International SMIRT Conference, Chicago, IL, August 22-26, 1983.
4. E. C. Lemmon, *COUPLE/FLUID A Two-Dimensional Finite Element Thermal Conduction and Advection Code*, EGG-ISD-SCD-80-1, February 1980.
5. J. Rest and S. A. Zawadzki, "FASTGRASS-VFP/PARAGRASS-VFP Version 50531, Users Guide," Argonne National Laboratory Quarterly Report, January-March 1983, Volume I, NUREG/CR-3689, ANL-83-85 Volume I, June 1983.
6. *PATRAN Plus User's Manual*, Release 2.4, PDA Engineering, Costa Mesa, California 1987.
7. *ABAQUS User's Manual*, Version 4.6, Hibbitt, Karlsson & Sorensen, Inc., Providence, RI, 1987.
8. D. M. Snider, K. L. Wagner, W. Grush, *Nuclear Plant Analyzer (NPA) Reference Manual Mod1*, EGG-EAST-9096, April 1990.
9. K. D. Bergeron et al., *User's Manual for CONTAIN 1.0, A Computer Code for Severe Nuclear Reactor Accident Containment Analysis*, NUREG/CR-4085, SAND84-1204, May 1985.
10. L. T. Ritchie et al., *CRAC2 Model Description*, NUREG/CR-2552, SAND82-0342, March 1984.
11. D. I. Chanin et al., *MELCOR Accident Consequence Code System (MACCS Version 1.5)*, NUREG/CR-4691, SAND86-1562, July 1988, DRAFT.
12. J. W. Spore et al., *TRAC-BD1: An Advanced Best Estimate Computer Program for Boiling Water Reactor Loss of Coolant Accident Analysis*, NUREG/CR-2178, EGG-2109, October 1981.
13. J. W. Spore, M. M. Giles, and R. W. Shumway, "A Best Estimate Radiation Heat Transfer Model Developed for TRAC-BD1," ASME Paper No. 80-HT-68, 20th Joint ASME/AIChE National Heat Transfer Conference, Milwaukee, WI, August 1981.
14. C. J. Shaffer, "Importance of Thermal Radiation to Steam in Rod Bundles," Topical Meeting on Water Reactor Safety, Salt Lake City, UT, March 26-28, 1973, pp. 371-379.
15. D. A. Mandell, *A Radiative Heat Transfer Model for the TRAC Code*, NUREG/CR-0994, LA-7965-MS, November 1979.
16. J. G. M. Anderson et al., *NORCOOL I, A Model for the Analysis of a BWR Under LOCA Conditions*, NORHAV-D-47, August 1977.
17. J. G. M. Anderson and H. Abel-Larsen, *CORECOOL Model Description of the Programme*, RISO-M-2138, November 1978.
18. J. G. M. Anderson and C. L. Tien, "Radiation Heat Transfer in a BWR Fuel Bundle Under LOCA Conditions," Fluid Flow and Heat Transfer Over Rod or Tube Bundles, S. C. Yao and P. A. Pfund eds., ASME, New York, NY, 1979, pp. 197-207.
19. K. H. Sun, J. M. Gonzales-Santalo, and C. L. Tien, "Calculations of Combined Radiation and Convection Heat Transfer in Rod Bundle Under Emergency Cooling Conditions," Journal of Heat Transfer, 98, 1976, pp. 414-420.

## References

20. R. Siegel and J. R. Howell, *Thermal Radiation Heat Transfer*, New York: McGraw-Hill Book Company, 1972.
21. E. M. Sparrow and R. D. Cess, *Radiation Heat Transfer*, Belmont: Brooks/Cole Publishing Company, 1966.
22. R. L. Cox, *Radiative Heat Transfer in Arrays of Parallel Cylinders*, ORNL-5239, June 1977.
23. D. A. Mandell, "Geometric View Factors for Radiative Transfer Within Boiling Water Reactor Fuel Bundles," *Nuclear Technology*, 52, 1981, pp. 383-392.
24. D. R. Evans, *The MOXY Digital Computer Program for Boiling Water Reactor Core Thermal Analysis*, RE-A-77-081, September 1981.
25. N. H. Juul, "View Factors in Radiation Between Two Parallel Oriented Cylinders of Finite Lengths," *Journal of Heat Transfer*, 104, 1982, pp. 384-388.
26. H. C. Hottel and A. F. Sarofim, *Radiative Transfer*, New York: McGraw-Hill Book Company, 1967.
27. *ENDF/B-V Library Tape 511 MATNO-1395*, National Neutron Cross Section Center, Brookhaven National Laboratory, July 1979.
28. "American National Standard for Decay Heat Power in Light Water Reactors", ANSI/ANS-5.1-1979.
29. B. G. Schnitzler, *Fission Product Decay Heat Modeling for Disrupted Fuel Regions (GDECAY)*, EGG-PHYS-5698, December 1981.